



Elettra Sincrotrone Trieste

Chemical and magnetic imaging with x-ray photoemission electron microscopy (XPEEM)

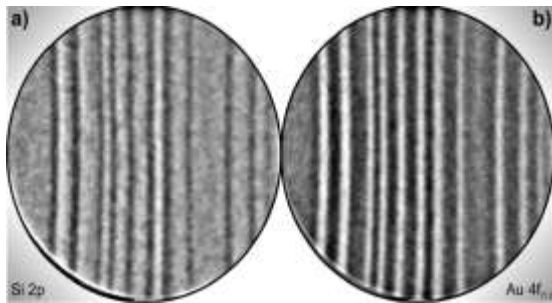
Andrea Locatelli

Andrea.locatelli@elettra.eu

Why do we need photoelectron microscopy?

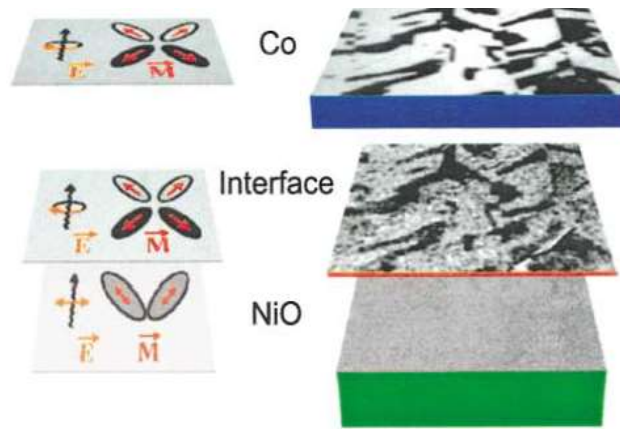
- To combine SPECTROSCOPY and MICROSCOPY to characterise the structural, chemical and magnetic properties of surfaces, interfaces and thin films
- Applications in diverse fields such as surface science, catalysis, material science, magnetism but also geology, soil sciences, biology and medicine.

Surface Science



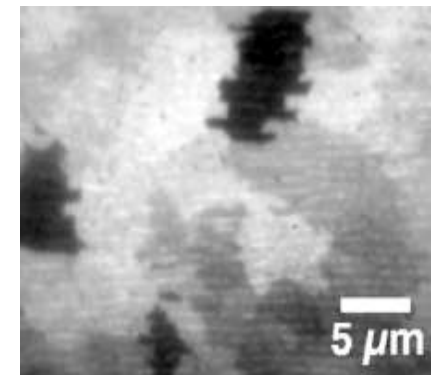
DOI: 10.1103/PhysRevLett.86.5088

Magnetism



DOI: 10.1103/PhysRevLett.87.247201

Biology



PRL 98, 268102 (2007)

- Synchrotron radiation and x-ray spectro-microscopy: basics
- Cathode lens microscopy: methods
- Applications
 - Chemical imaging of micro- structured materials
 - Graphene research.
 - Biology
 - Magnetism
 - Time-resolved XPEEM

Why does PEEM need synchrotron radiation?



Elettra Sincrotrone Trieste

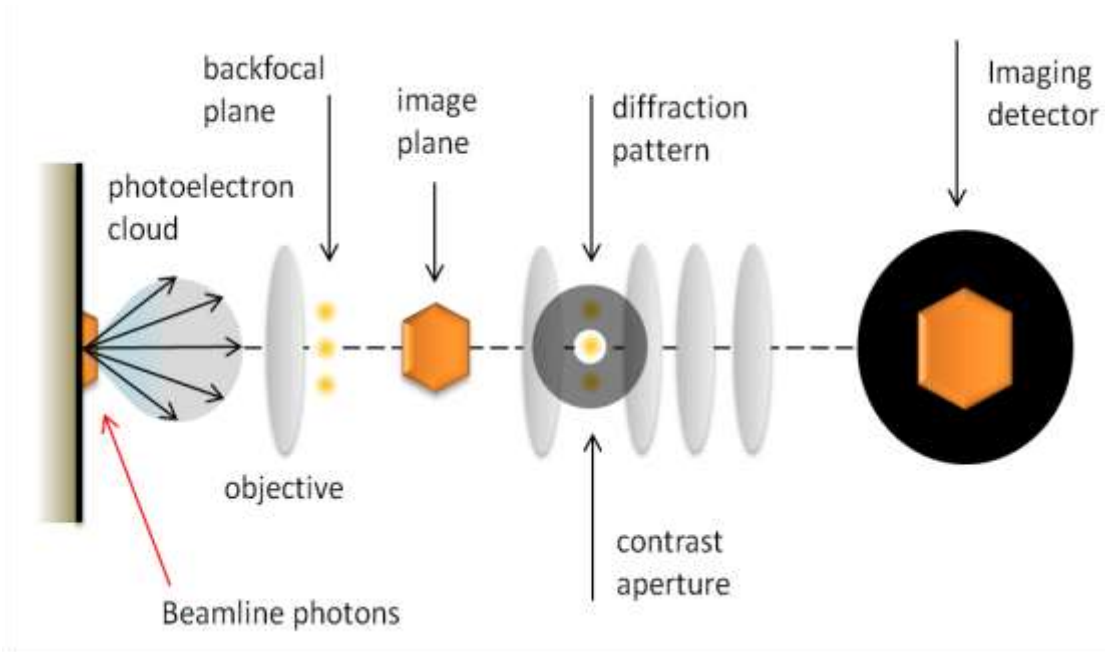
- **High intensity** of SR makes measurements faster
- **Tuneability** – very broad and continuous spectral range from IR to hard X-Rays
- Narrow angular collimation
- Coherence!
- **High degree of polarization**
- **Pulsed time structure** of SR – This adds time resolution to photoelectron spectroscopy!
- Quantitative control on SR parameters allows spectroscopy:
 - Absorption Spectroscopy (XAS and variants)
 - Photoemission Spectroscopies (XPS, UPS, ARPES, ARUPS)

$$J = f(h\nu, \varepsilon, \Theta, \Phi; E_{kin}^e, \sigma, \theta_e, \varphi_e)$$



Cathode lens microscopy methods

PEEM, LEEM, SPELEEM, AC-PEEM/LEEM



- Direct imaging, parallel detection
- Lateral resolution determined by electron optics: with AC, few nm possible
- Elemental sensitivity (XAS)
- Spectroscopic ability (energy filter)
- $P_{\max} < 5 \cdot 10^{-5}$ mbar

PEEM is a full-field technique. The microscope images a restricted portion of the specimen area illuminated by x-ray beam. Photoemitted electrons are collected at the same time by the optics setup, which produces a magnified image of the surface. The key element of the microscope is the objective lens, also known as cathode or immersion lens, of which the sample is part

Cathode lens operation principle



Elettra Sincrotrone Trieste

1. In emission microscopy θ (emission angle) is large. Electron lenses can accept only small θ because of large chromatic and spherical aberrations

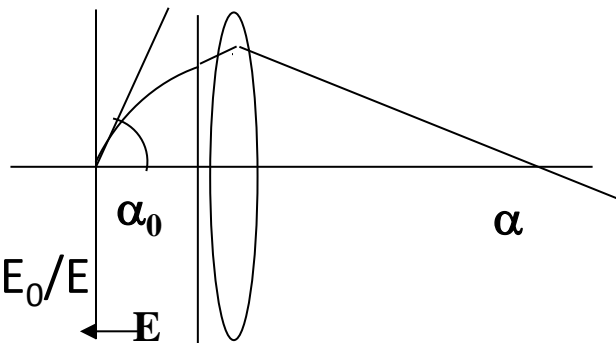
2. Solution of problem: accelerate electrons to high energy before lens \rightarrow Immersion objective lens or cathode lens

$$n \sin \theta = \text{const}$$

$$n \sim \sqrt{E}$$

$$\theta \rightarrow \alpha$$

$$\sin \alpha / \sin \alpha_0 = \sqrt{E_0 / E}$$

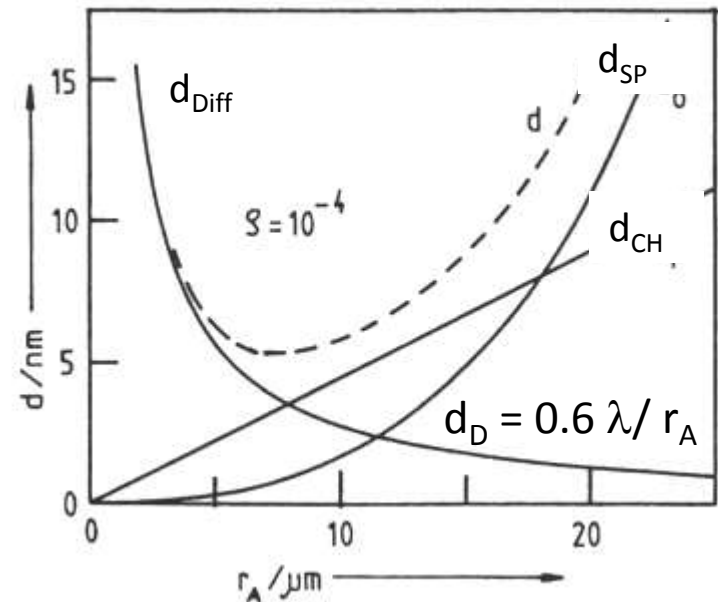


Example for $E = 20000 \text{ eV}$:

E_0	2 eV	200 eV
α for $\alpha_0 = 45^\circ$	0.4°	4.5°

3. The aberrations of the objective lens and the contrast aperture size determine the lateral resolution

$$d = \sqrt{d_{SP}^2 + d_{CH}^2 + d_D^2}$$



The different types of PEEM measurements



Elettra Sincrotrone Trieste

PEEM

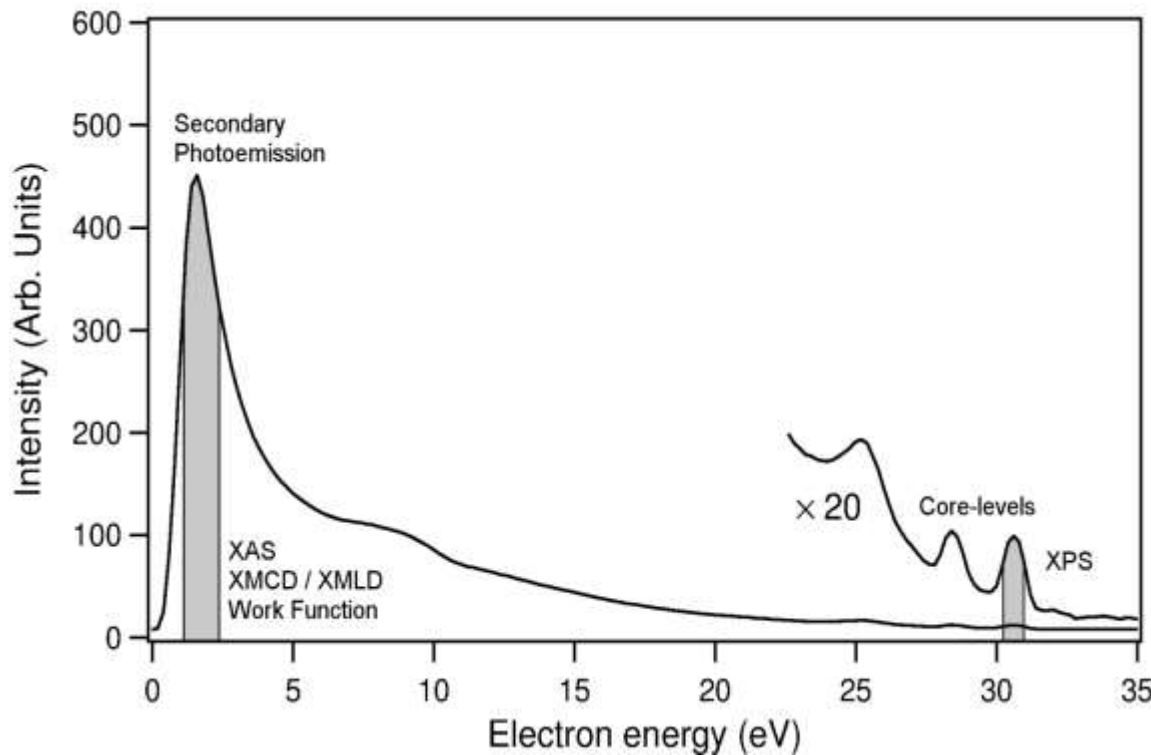
- threshold microscopy
- Laterally resolved XPS, micro-spectroscopy
- Laterally resolved UPS, microprobe ARUPS /ARPES
- Auger Spectroscopy
- XAS-PEEM (XMC/LD-PEEM)

Probe

- Hg lamp
- X-ray
- X-rays, He lamp
- X-ray, or electrons
- X rays

Measurement

- photoelectrons
- core levels or VB ph.el.
- VB photoelectrons
- secondary electrons
- secondary electrons

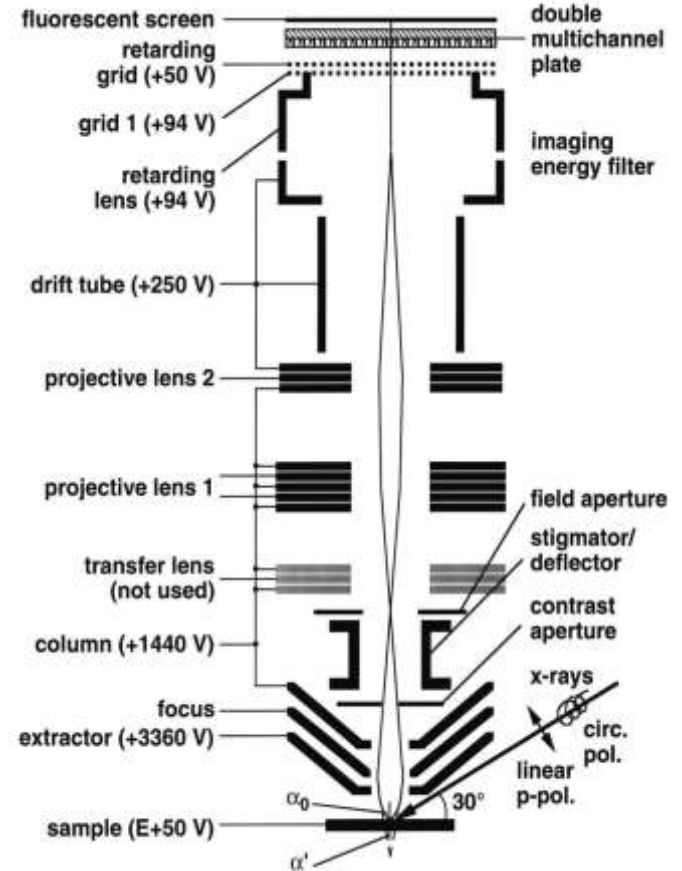
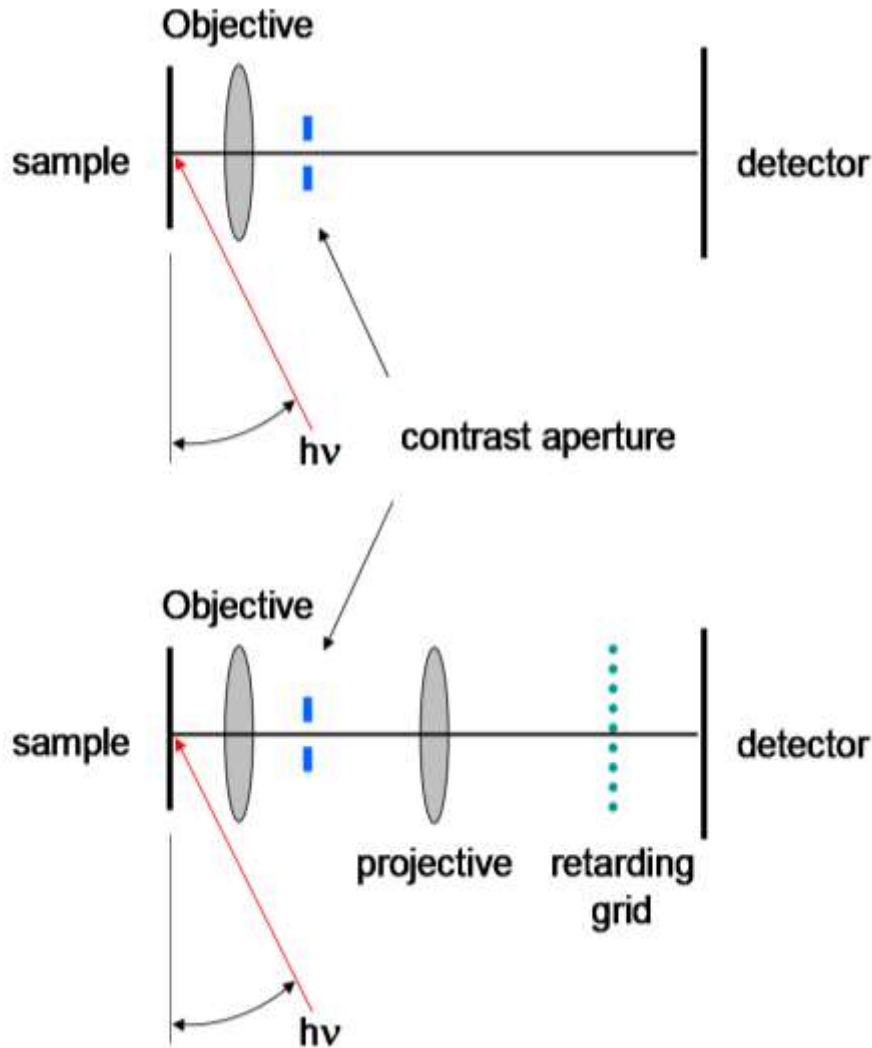


Require energy filter

Simple PEEM instruments



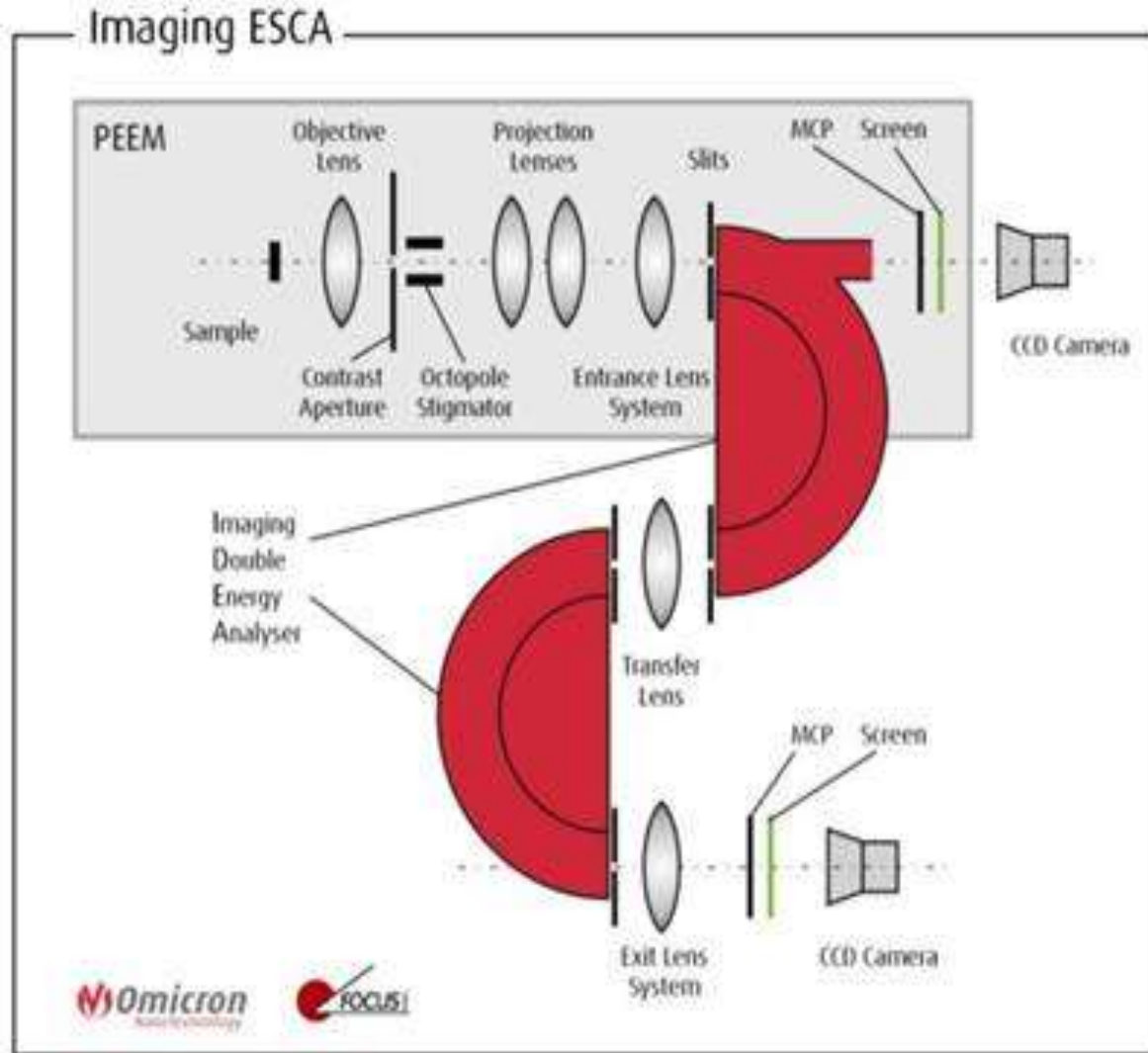
Elettra Sincrotrone Trieste



PEEM instruments with energy filter: NanoESCA

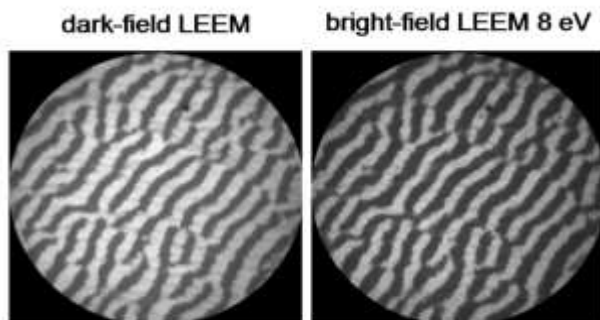


Elettra Sincrotrone Trieste

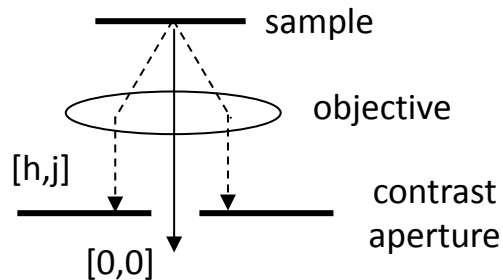


Different contrast mechanisms are available for structure characterization

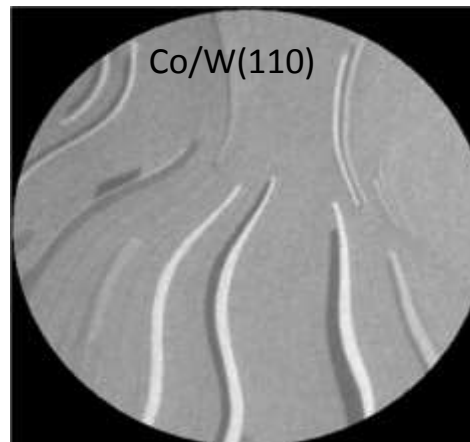
SURFACE STRUCTURE



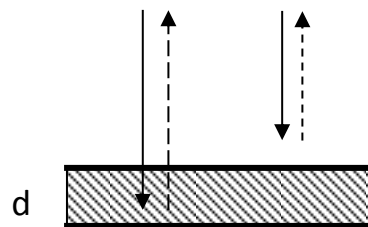
diffraction
contrast



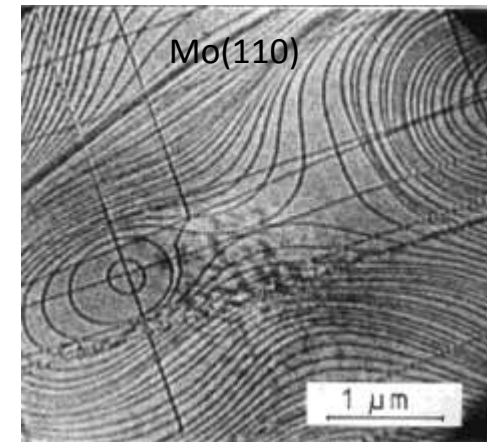
FILM THICKNESS



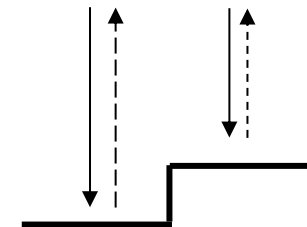
quantum size
contrast



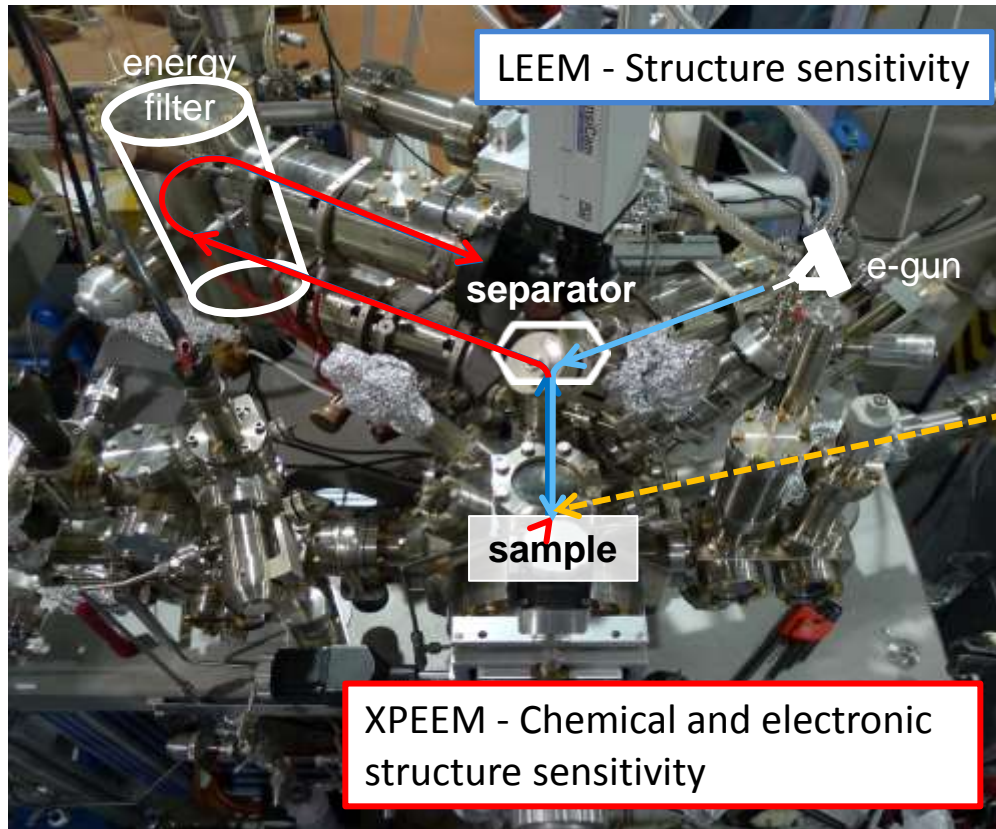
STEP MORPHOLOGY



geometric
phase contrast

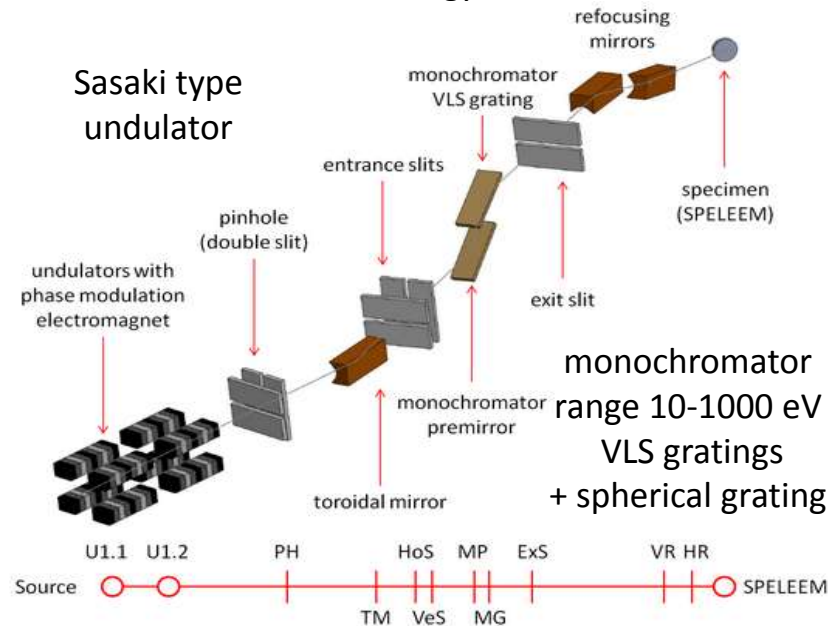


SPELEEM = LEEM + PEEM



The Nanospectroscopy beamline@Elettra

Flux on the sample: 10^{13} ph/sec (microspot)
intermediate energy resolution.



Applications:

characterization of materials at microscopic level, magnetic imaging of micro-structures
Imaging of dynamical processes

A. Locatelli, L. Aballe, T.O. Menteş, M. Kiskinova, E. Bauer, Surf. Interface Anal. 38, 1554-1557 (2006)

T. O. Menteş, G. Zamborlini, A. Sala, A. Locatelli; Beilstein J. Nanotechnol. 5, 1873-1886 (2014)

SPELEEM many methods analysis

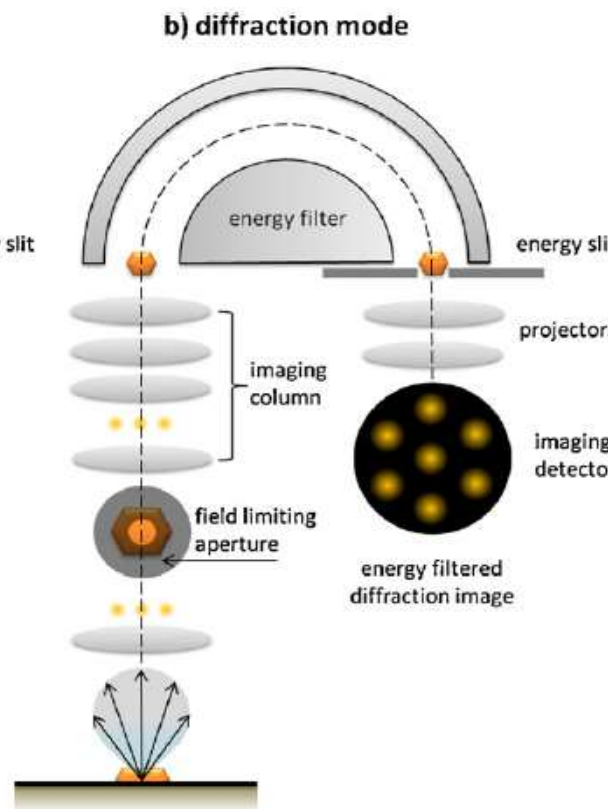
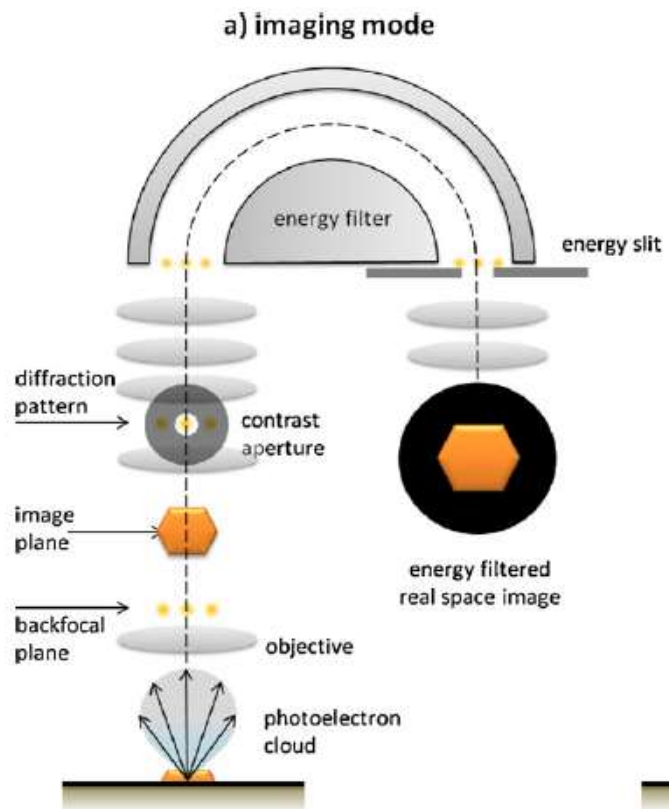


Elettra Sincrotrone Trieste

Spectroscopic imaging
XAS-PEEM / XPEEM / LEEM

microprobe-diffraction
ARPES / LEED

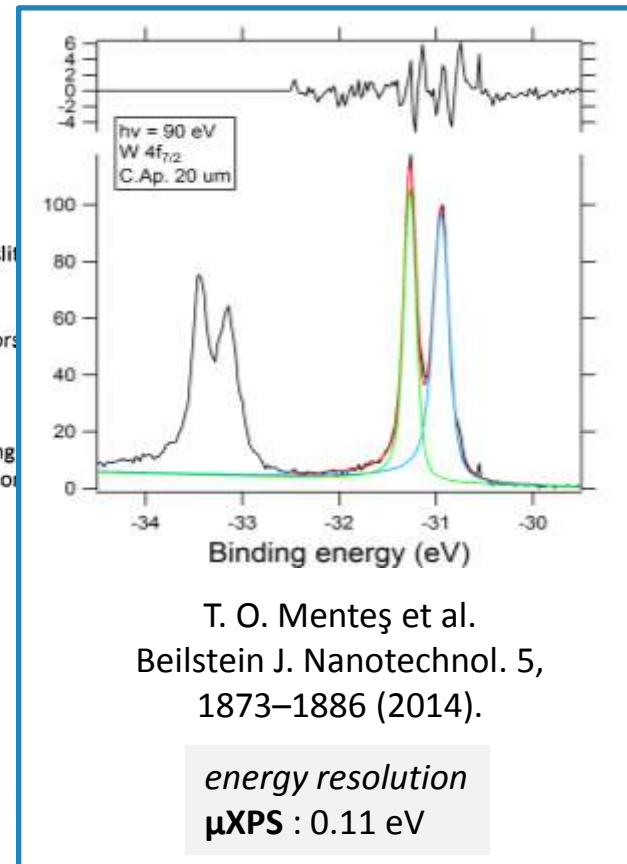
microprobe-spectroscopy
XPS



spatial resolution
LEEM : 10 nm
XPEEM : 25 nm

energy resolution
XPEEM : 0.3 eV

Limited: to 2 microns in dia.
angular resolution
transfer width: 0.01 \AA^{-1}



Performance: lateral resolution in imaging: **10nm** (LEEM)
30 nm (XPEEM)
energy resolution: **0.3 eV** (0.1 eV muXPS)

Key feature: multi-method instrument to the study of surfaces and interfaces offering *imaging* and *diffraction* techniques.

Probe: *low energy e-* (0-500 eV) \longleftrightarrow structure sensitivity
soft X-rays (50-1000 eV) \longleftrightarrow chemical state, magnetic state, electronic struct.

Applications: *characterization* of materials at microscopic level
magnetic imaging of microstructures
dynamical processes

Correction of spherical and chromatic aberrations



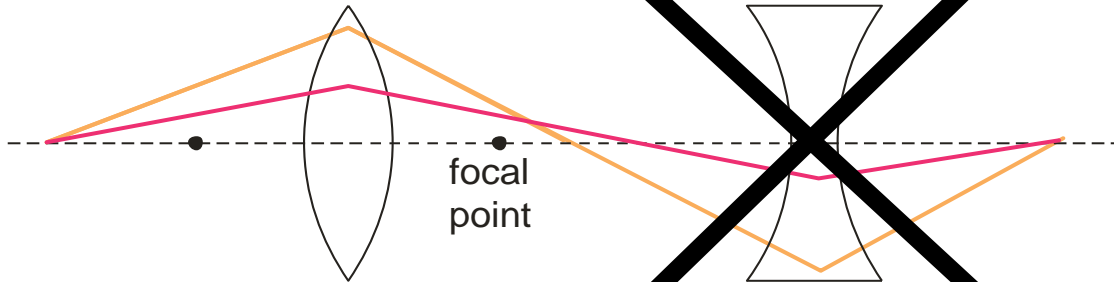
Elettra Sincrotrone Trieste

Electron optics

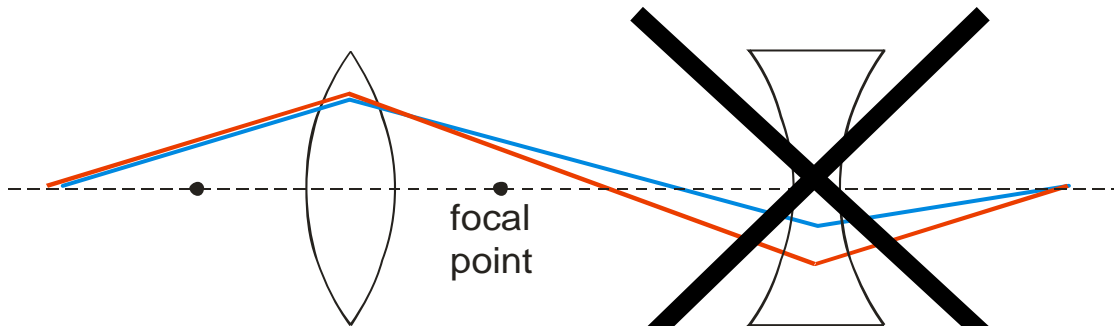
Round **convex** lenses

Round **concave** lenses

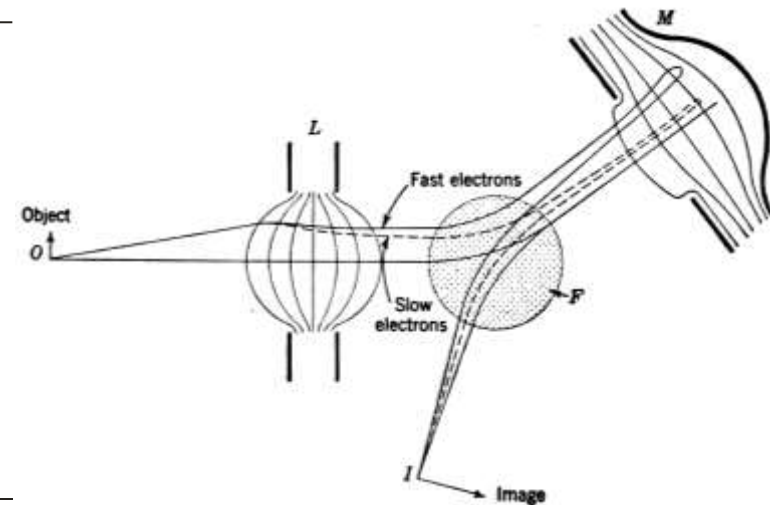
Electron Mirror



Spherical aberration



Chromatic aberration



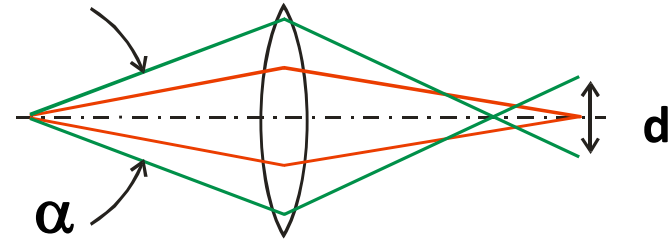
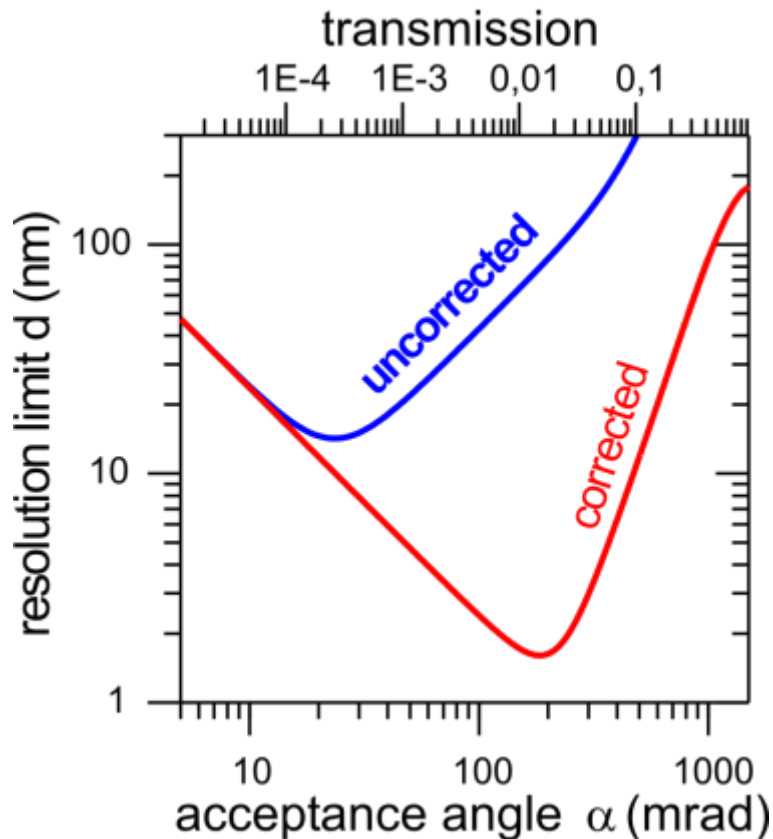
V.K. Zworykin et al, Electron Optics and the Electron Microscope, John Wiley, New York 1945

The SMART AC microscope: calculation



Elettra Sincrotrone Trieste

Simultaneous improvement in Transmission and Resolution!!!



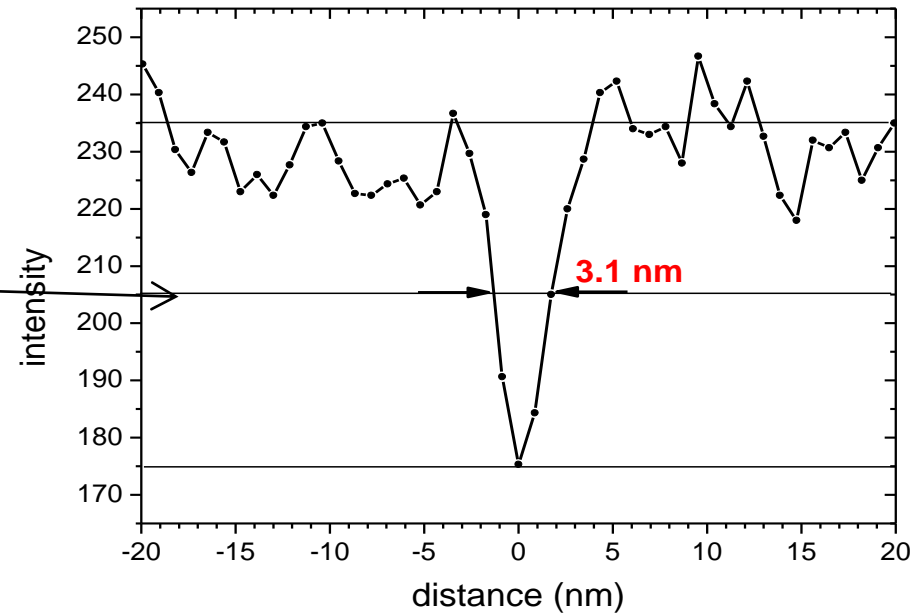
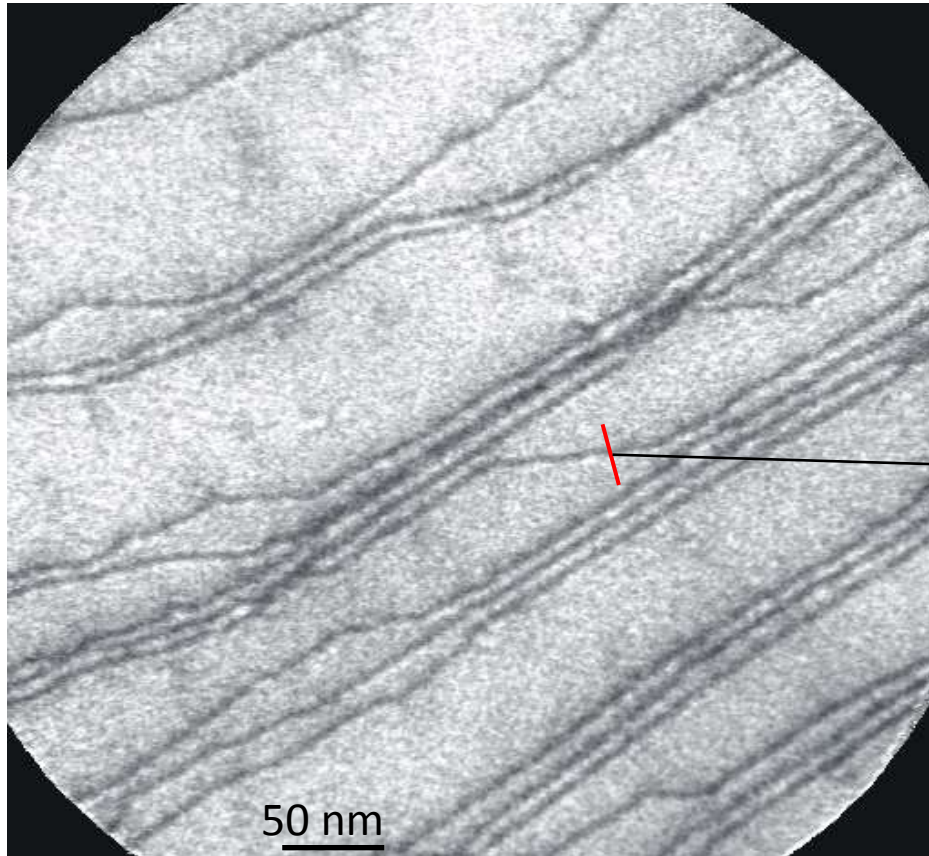
Resolution limit	without correction	with correction
Spherical	$\alpha^3 + \dots$	α^5
Chromatic	$\Delta E \alpha + \dots$	$\Delta E \alpha^2 + \Delta E^2 \alpha$
Diffraction	$1/\alpha$	$1/\alpha$

D. Preikszas, H. Rose, J. Electr. Micr. 1 (1997) 1

Th. Schmidt, D. Preikszas, H. Rose et al., Surf.Rev.Lett 9 (2002) 223

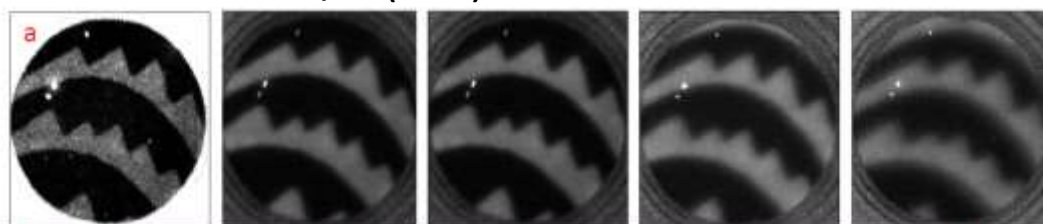
First results of the SMART microscope @BESSY

Atomic steps on Au(111),
LEEM 16 eV, FoV = 444 nm x 444 nm
(18.09.06)

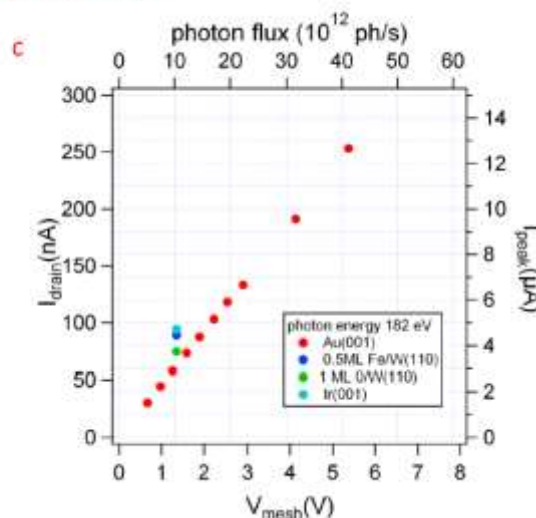
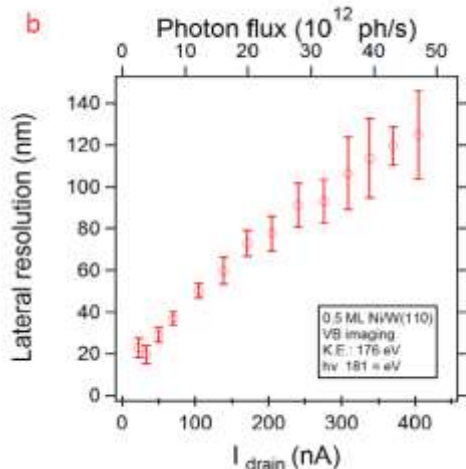


Courtesy of Th. Schmidt et al.; 5th Int. Conf. LEEM/PEEM, Himeji, 15.-19. Oct. 2006

Ni/W(100) $h\nu = 181$ eV



Increasing photon flux →



photocurrent estimate for
SPELEEM@Elettra; Au/W(110)

- 440 bunches
rev. frequency: 1.157 MHz
bunch length: 42 ps (2GeV)
- $1 \cdot 10^{13}$ ph./s on sample =
= 20000 ph./bunch
- Total photoionization yield:
about 2% photons result in a
photoemission event
- $I_{\text{peak}} \approx 400 \text{ e}^- / 42 \text{ ps}$
 $\approx 1.5 \mu\text{A}$ vs 20 nA (LEEM)
13 pA/ μm^2 versus 20 nA/ μm^2

1. Image blur can be observed with SR but only under very high photon fluxes. Must Keep into account in beamline design. No space charge in LEEM
2. Both the lateral and energy resolution are strongly degraded by Boersch and Loeffler effects occurring in the first part of optical path.



Chemical imaging applications

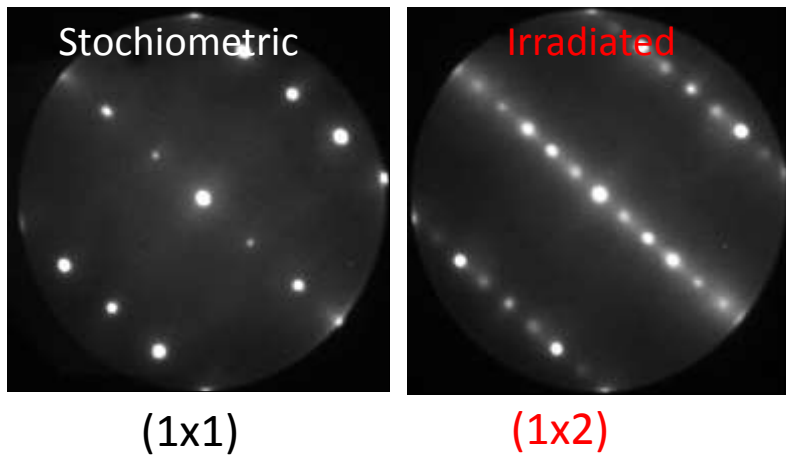
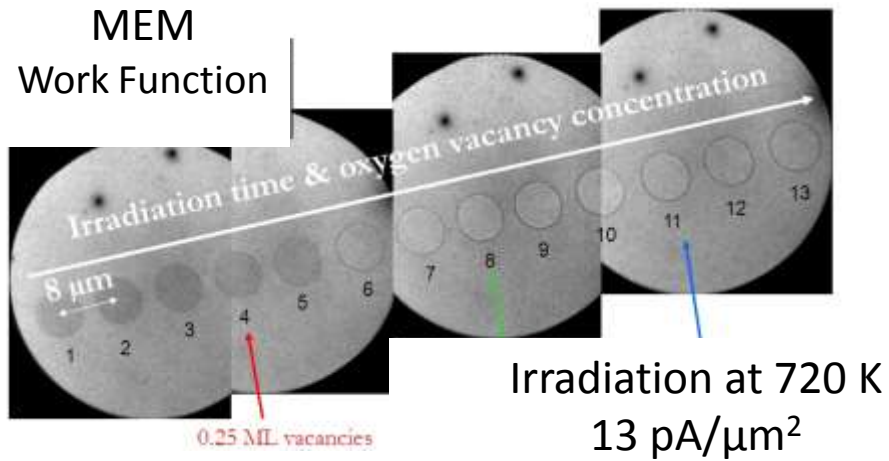
PEEM, LEEM, SPELEEM, AC-PEEM/LEEM

Au/TiO₂(110): controlling growth by vacancies

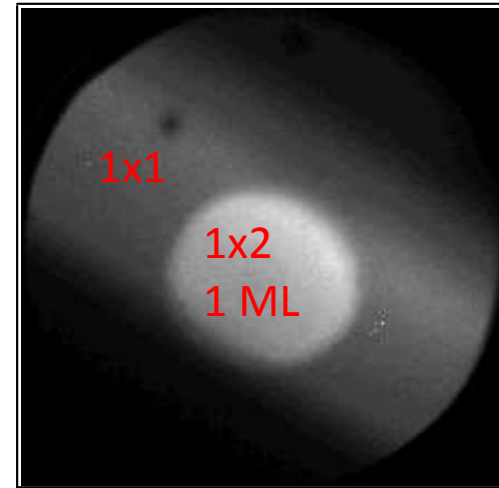


Elettra Sincrotrone Trieste

Creation of ordered oxygen vacancies

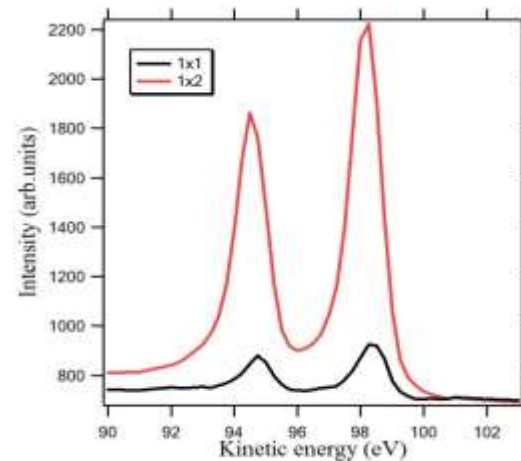


Au growth on TiO₂(110)



XPEEM
@ Au 4f

μ -LEIS
struc



μ -XPS

Surface Oxygen on Ag : *e*-beam "Lithography"

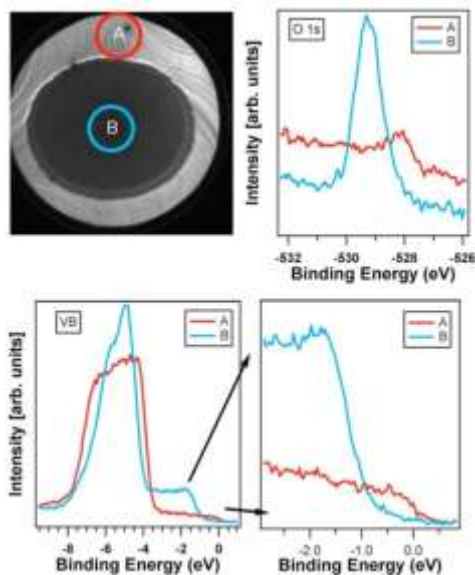


Elettra Sincrotrone Trieste

Full oxidation of Ag using NO₂ does not occur:



Instead: *e*-beam (60 eV) stimulated desorption of NO_{ad} works at RT!

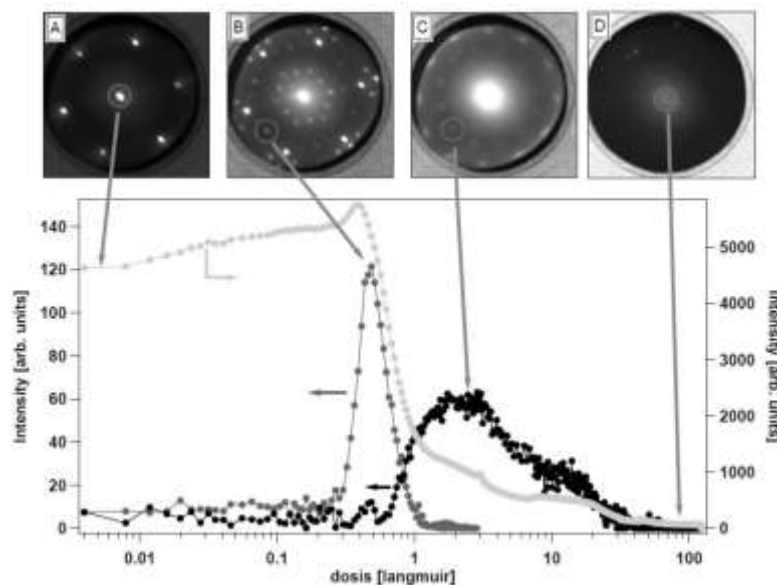


A: metallic Ag
B: Ag₂O

Low T: NO_{ad} stays, prevents oxidation.

High T: NO_{ad} desorbs, but Ag₂O unstable.

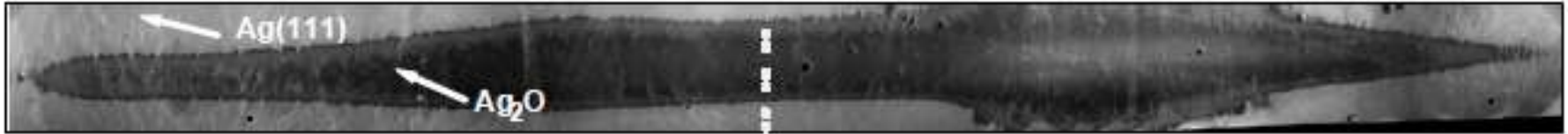
LEED reveals path towards Ag₂O under *e*-beam



S. Günther *et al.*, *App. Phys. Lett.* 93, 233117 (2008).

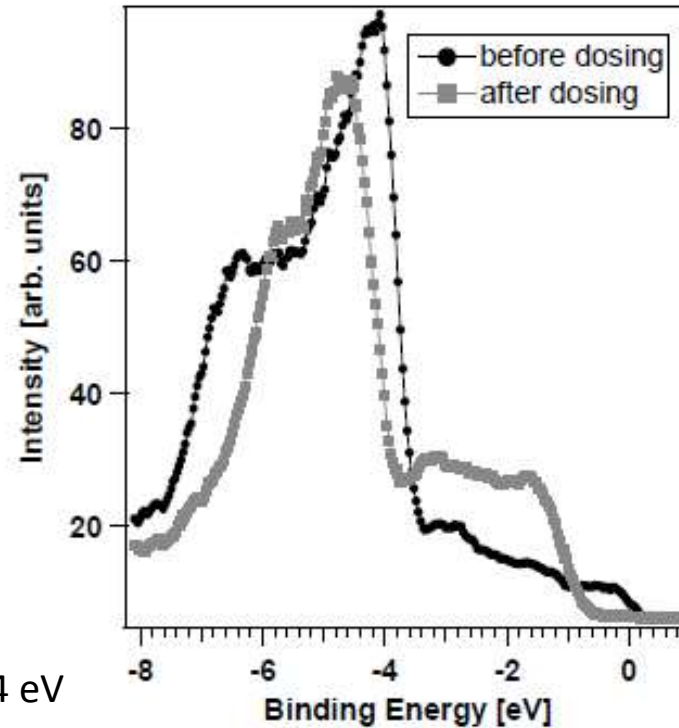
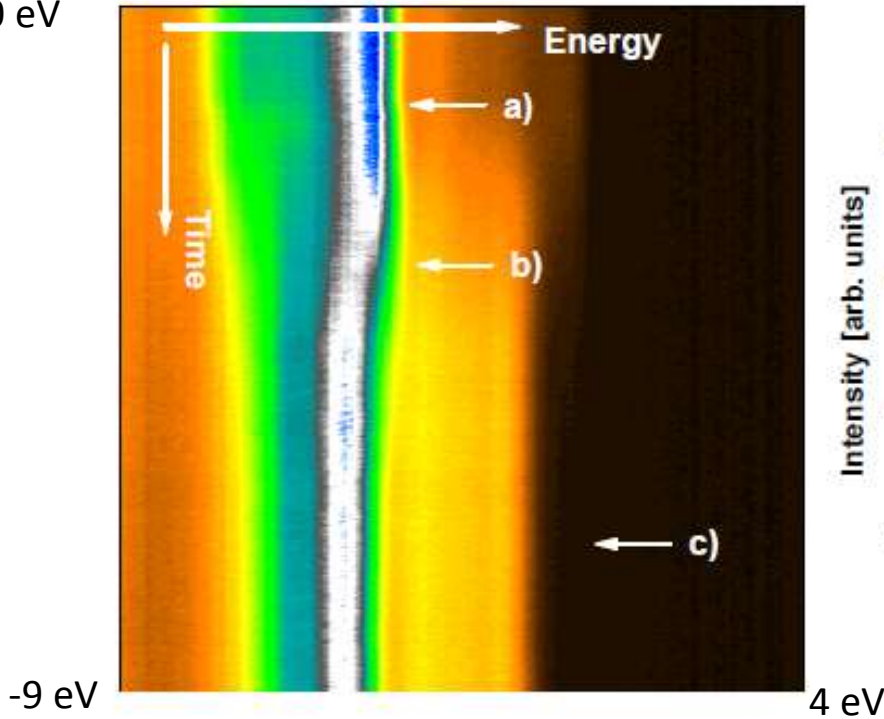
S. Günther *et al.*, *Chem. Phys. Chem.* 2010.

Surface Oxygen on Ag : photon-beam “Lithography”



MEM 28 μm x 350 μm ; after 130 L NO_2 ;

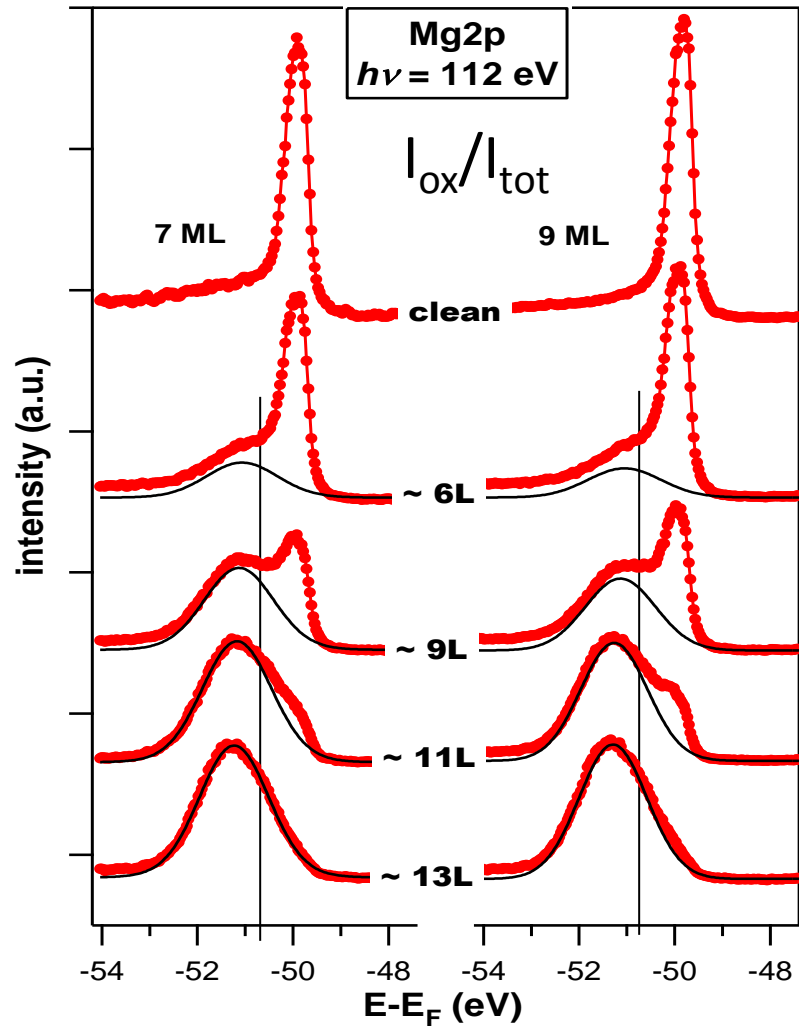
$h\nu = 40 \text{ eV}$



- (a) Start of NO_2 adsorption, $t = 0 \text{ s}$,
- (b) $t = 210 \text{ s}$, $p(\text{NO}_2) = 1.8 \times 10^{-7} \text{ mbar}$, 17 L NO_2 ,
- (c) $t = 540 \text{ s}$, $p(\text{NO}_2) = 2.5 \times 10^{-7} \text{ mbar}$, 67 L NO_2 .

S. Günther *et al.*, *Chem. Phys. Chem.* 2010.

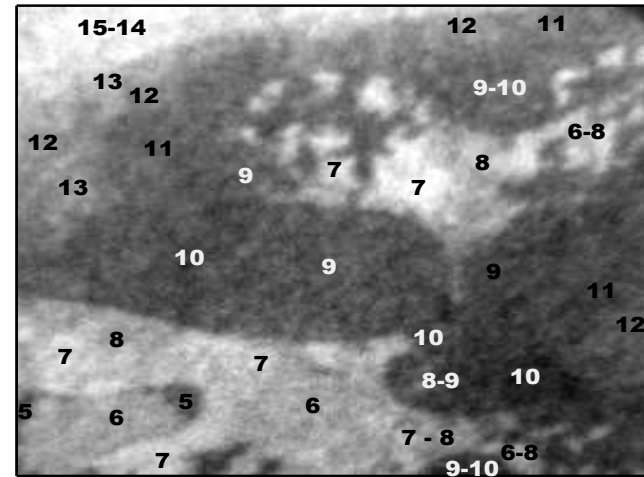
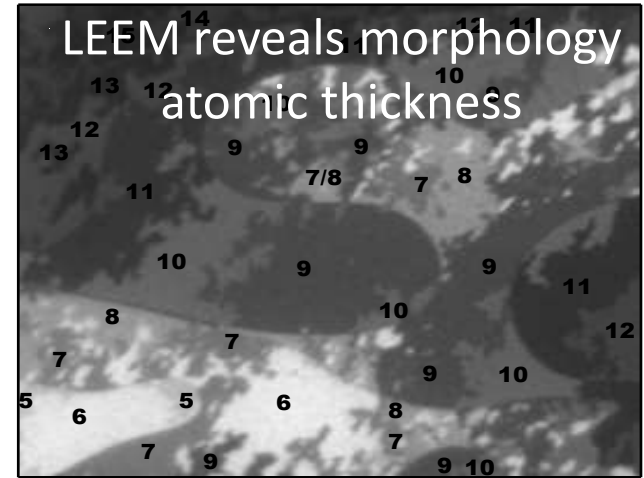
Thickness dependent reactivity in Mg



1 μm

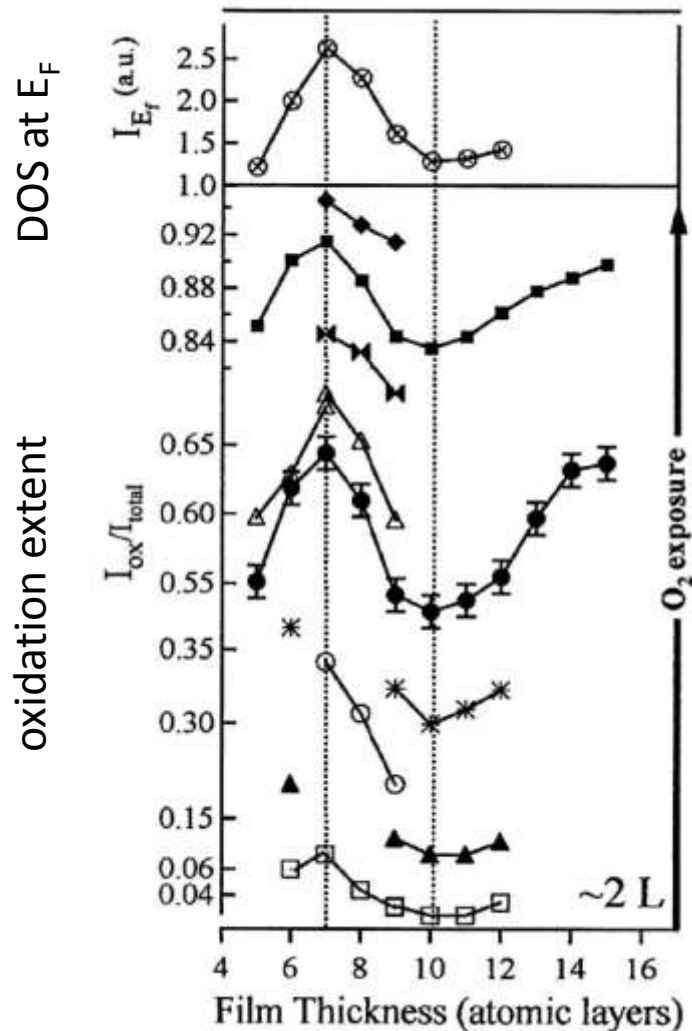
O_2 exposure

A vertical arrow pointing downwards, indicating the direction of increasing O_2 exposure. A scale bar at the top indicates a length of 1 μm .



Oxide component reveals chemistry!

L. Aballe *et al.*, Phys. Rev. Lett. **93**, 196103 (2004)



FACTS

- ✓ Strong variations in the oxidation extent are correlated to thickness and to the density of states at E_F
- ✓ XPEEM is a powerful technique for correlating chemistry and electronic structure information

SIGNIFICANCE OF THE EXPERIMENTS

- ✓ Control on film thickness enables modifying the molecule-surface interaction
- ✓ Theoretical explanation: Decay length of QWS into vacuum is critical: it reproduces peak of reactivity in experimental data. See Binggeli and M. Altarelli, Phys.Rev.Lett. 96, 036805 (2005)

L. Aballe *et al.*, Phys. Rev. Lett. 93, 196103 (2004)

Spatiotemporal Concentration Patterns in a Surface Reaction: Propagating and Standing Waves, Rotating Spirals, and Turbulence

S. Jakubith, H. H. Rotermund, W. Engel, A. von Oertzen, and G. Ertl

Fritz-Haber-Institut der Max-Planck-Gesellschaft, Faradayweg 4-6, D-1000 Berlin 33, Germany

(Received 25 June 1990)

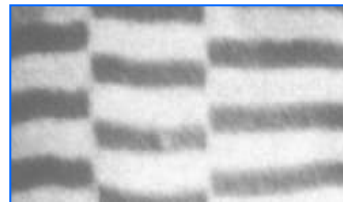


Belousov-Zabatinski reaction
(solution of, acidified bromate,
malonic acid, ceric salt)

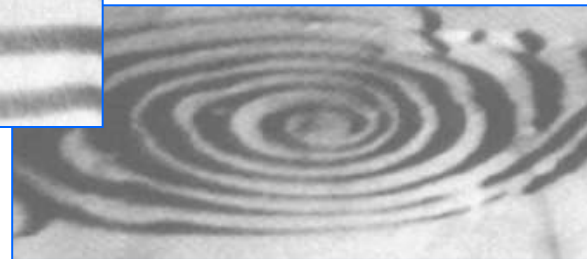
Pattern formation in surface chemical reactions

oscillatory oxidation of carbon monoxide
on a Pt(110) surface

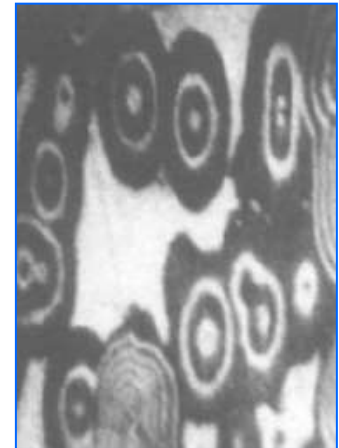
standing fronts



rotating spirals



target waves



Jakubith *et al.*, PRL 65, 3013 (1990)

See also: W. Engel, *et al.*, Ultramicroscopy **36**, 148–153 (1991).

Reaction diffusion patterns: NO+H₂ /Rh(110)

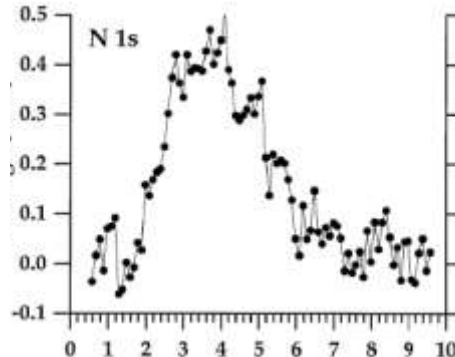
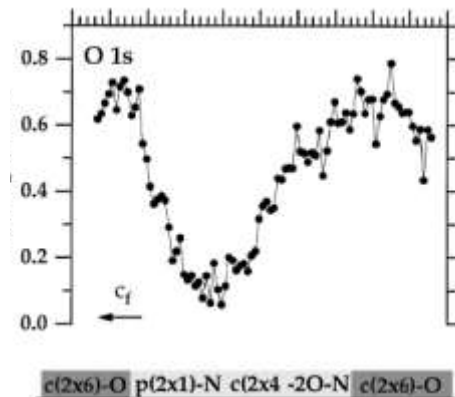
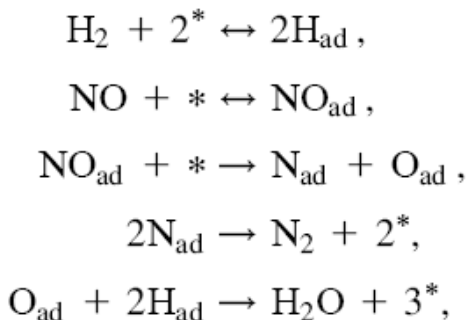
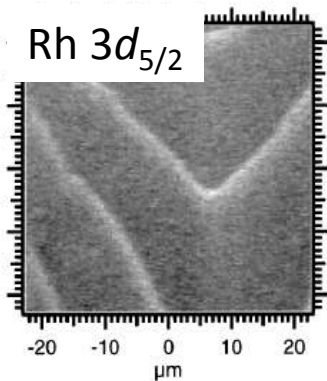
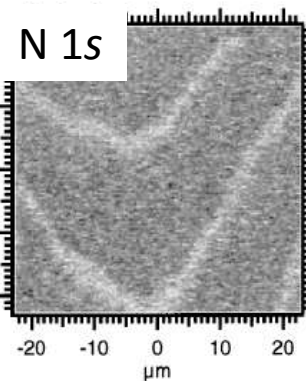
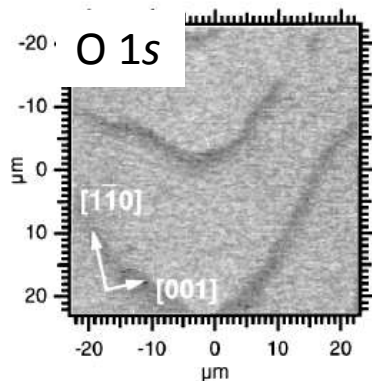
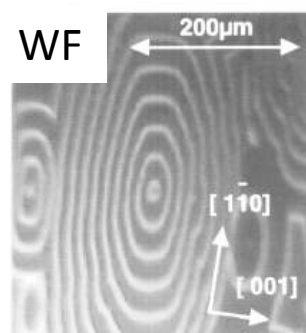


Elettra Sincrotrone Trieste

First quantitative measurements of concentration profiles by SPEM

Schaak et al

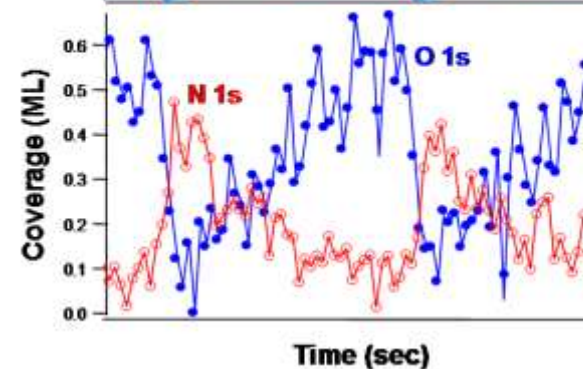
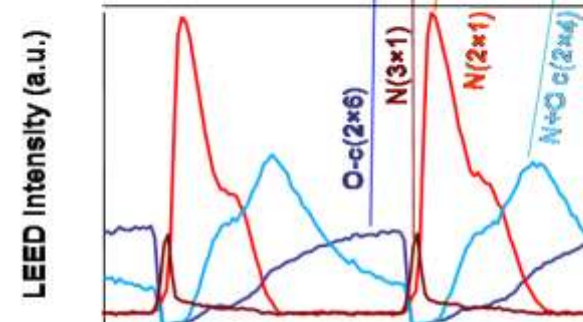
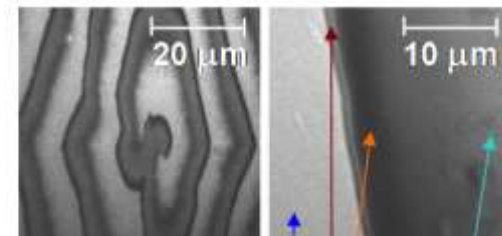
Phys. Rev. Lett. **83**, 1882 (1999)



LEEM, micro-LEED

Th. Schmidt *et al.*,

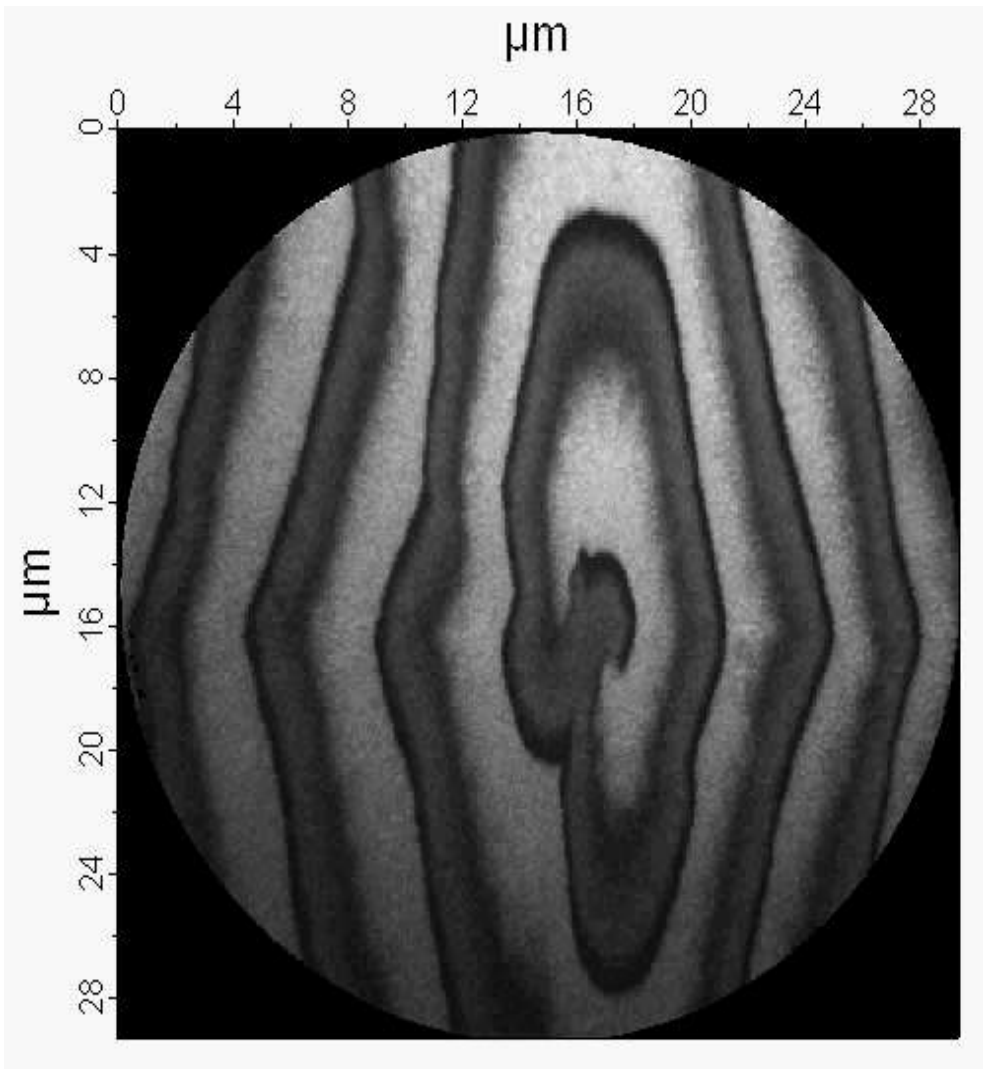
Chem. Phys. Lett. 318, 549 (2000)



Reaction diffusion patterns: NO+H₂ /Rh(110)

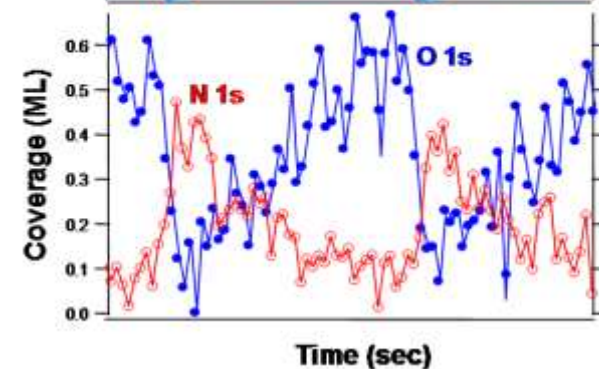
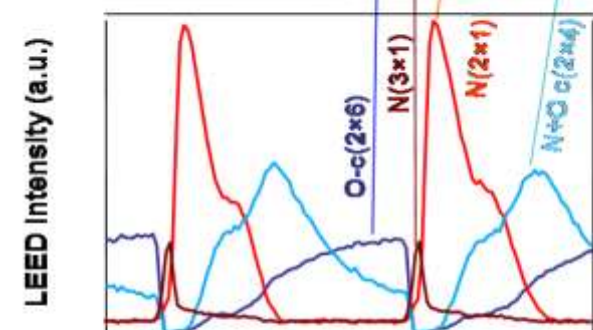
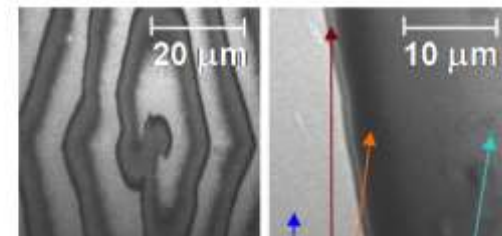


Elettra Sincrotrone Trieste



LEEM, micro-LEED

Th. Schmidt *et al.*,
Chem. Phys. Lett. 318, 549 (2000)



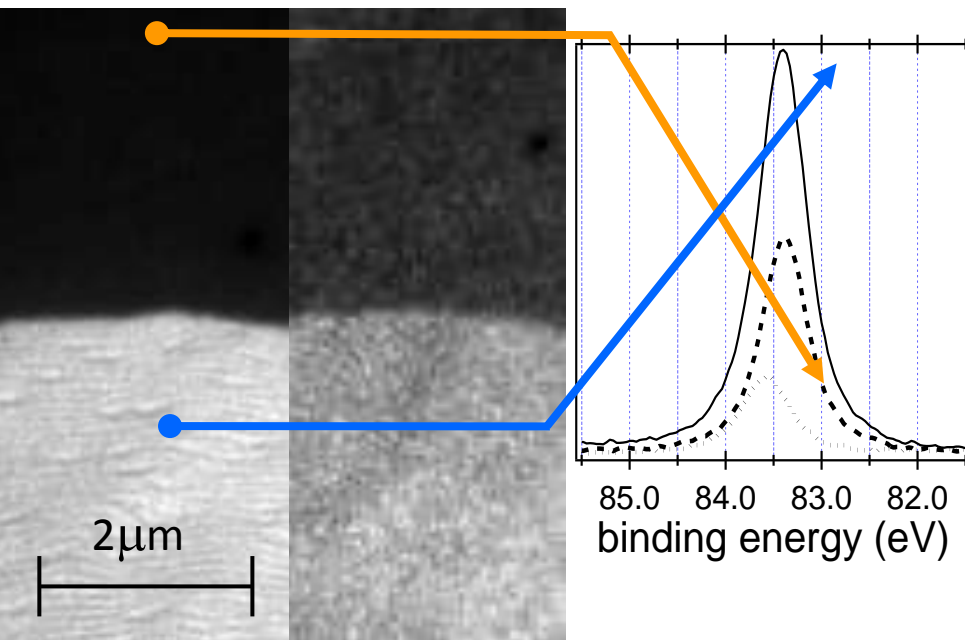
Reactive phase-separation processes



Elettra Sincrotrone Trieste

H₂+O₂/Au/Rh(110)

Spectroscopic determination of reaction induced redistribution



LEEM

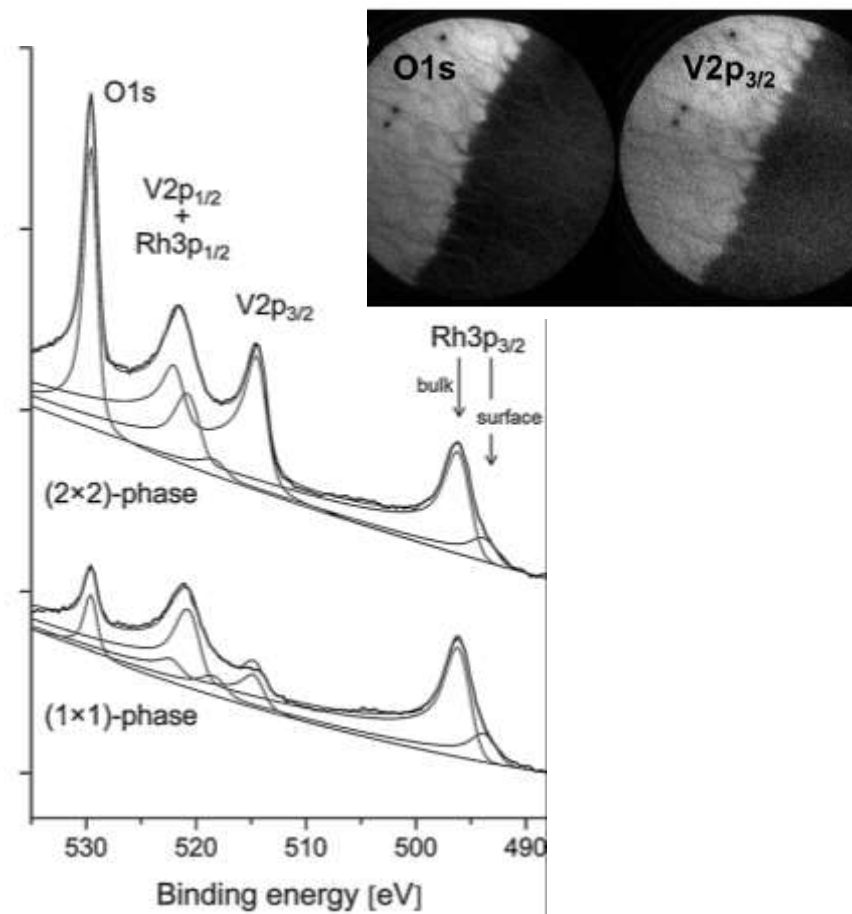
XPEEM
Au 4f_{7/2}

Surface Science 566–568 (2004) 1130–1136

J. AM. CHEM. SOC. 2005, 127, 2351–2357

V/Rh(110) during water formation reaction

Spectroscopic determination of the oxidation state



F. Lovis et al., *J. Phys. Chem. C* **115**, 19149 (2011)

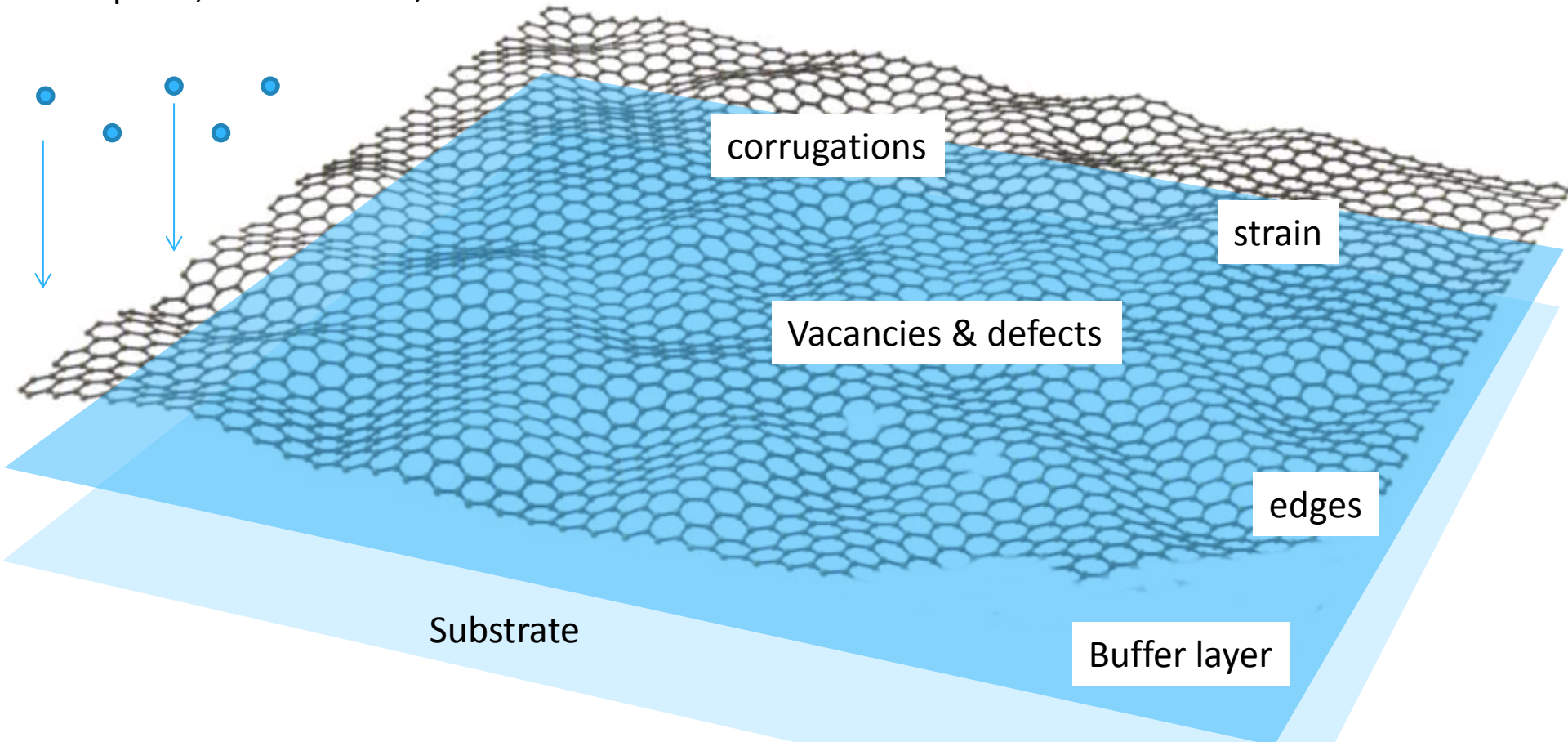
The complexity of the metal-graphene interface



Elettra Sincrotrone Trieste

adsorption, intercalation,

Irradiation, functionalization, implantation



- Understand and control the fundamental interactions occurring at the interface
- **verify the properties (crystal quality, stoichiometry, electronic structure) at the mesoscale!**

XPEEM studies of graphene

- Effect of substrate' symmetry
 - The complex structure of g/Ir(100)
- Buffers
 - Au Intercalation
 - Carbides in graphene on Ni(111)
- Irradiation/implantation
 - Low energy N⁺ ion irradiation of g/Ir(111)
 - Irradiation with noble gases of g/Ir(100)

High temperature graphene growth on Ir(100)



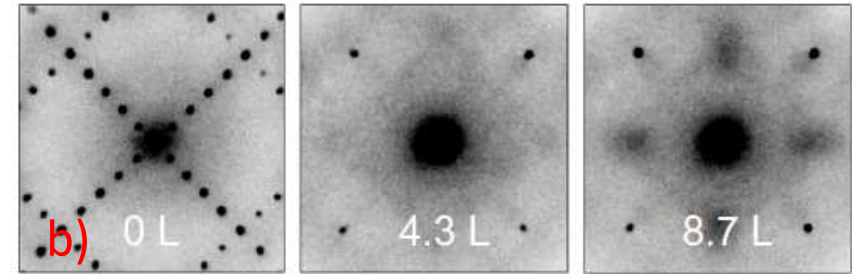
Elettra Sincrotrone Trieste

LEEM imaging

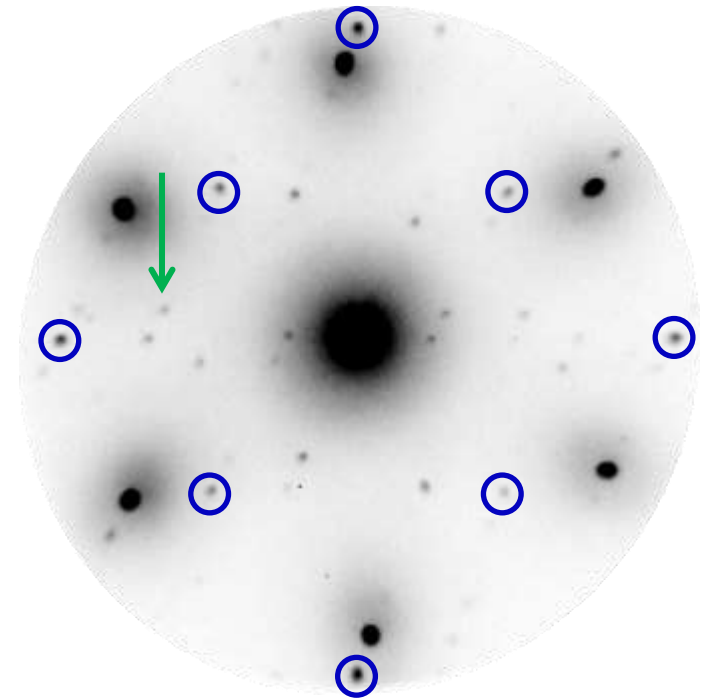


$T > 800 \text{ C}; P = 2 \cdot 10^{-8} \text{ mbar ethylene}$

microprobe-LEED: Ir



microprobe-LEED: graphene



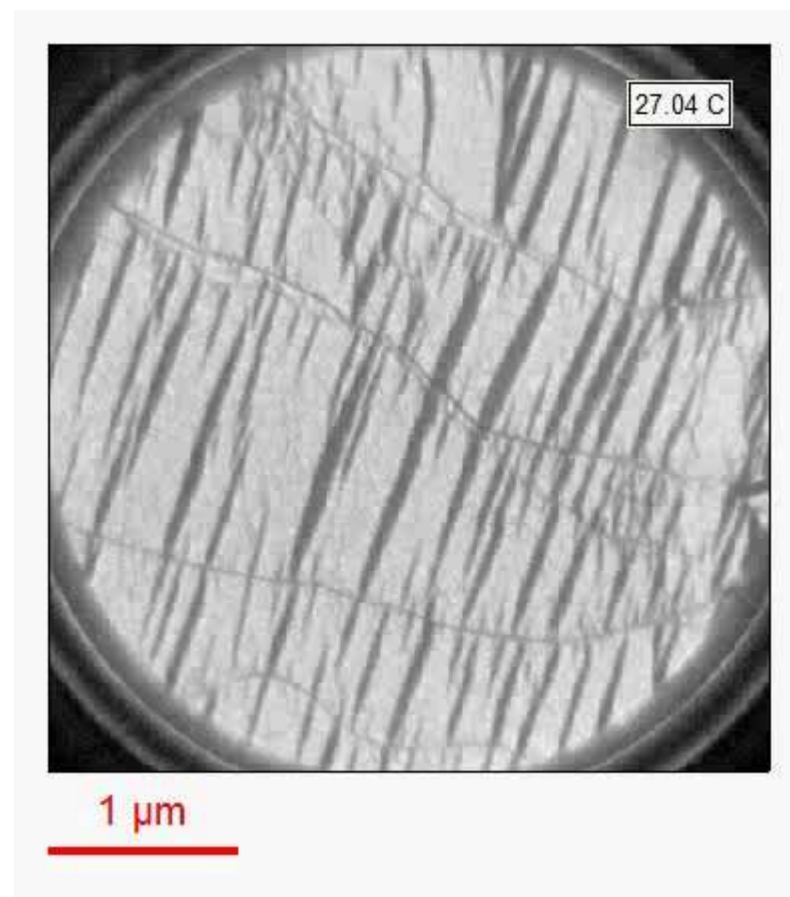
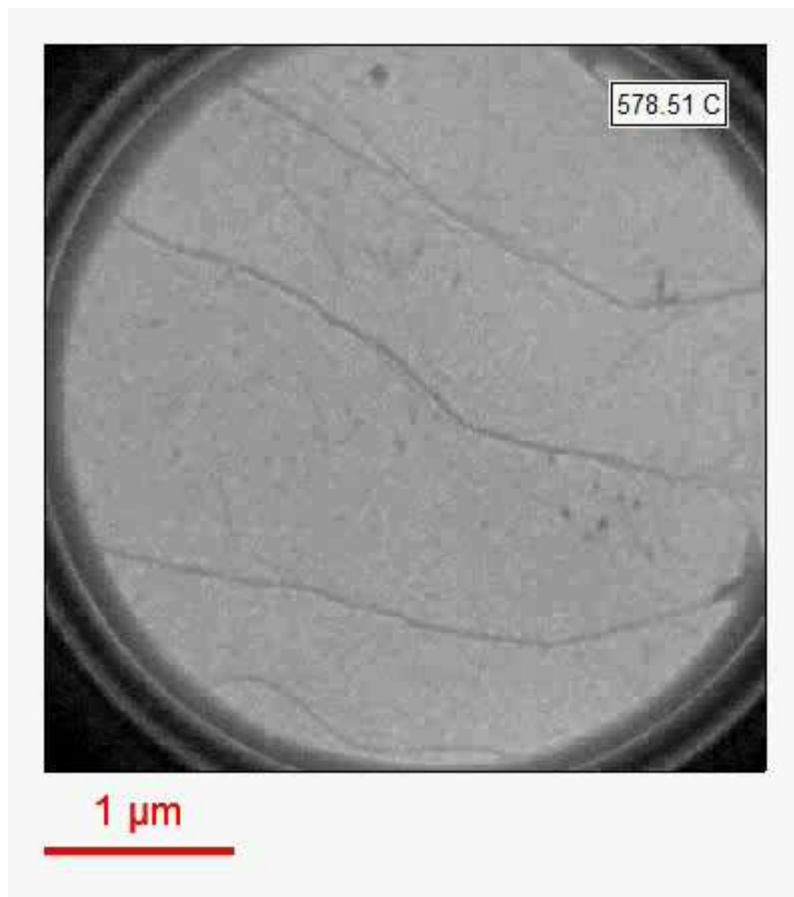
Reversible graphene phase transformation



Elettra Sincrotrone Trieste

Upon cooling a distinct graphene phase nucleates forming dark stripes

The stripes disappear when annealing the sample to high temperature.

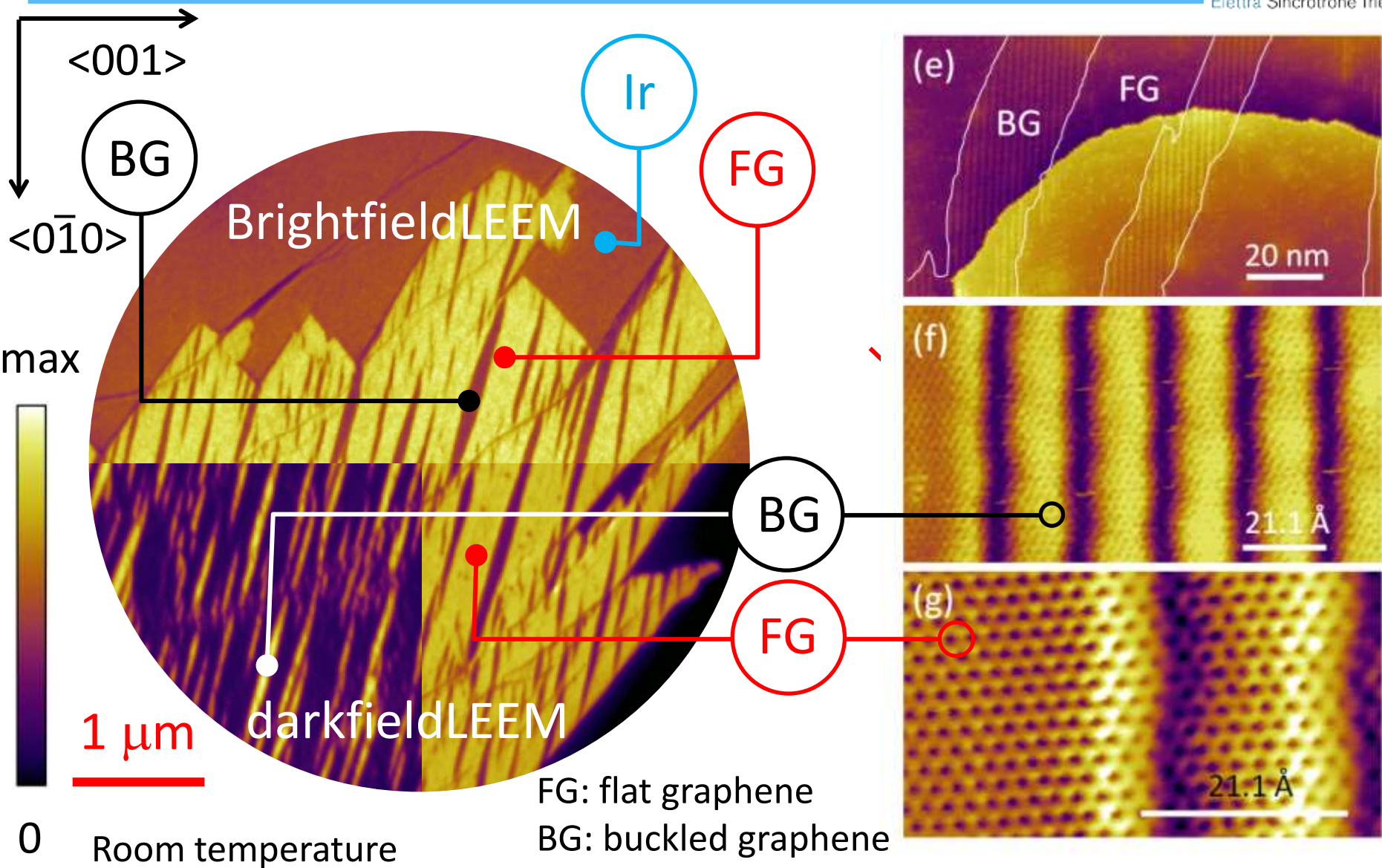


Fov 4 μm , S.V. 13 eV

Graphene/Ir(100): structure of FG and BG



Elettra Sincrotrone Trieste



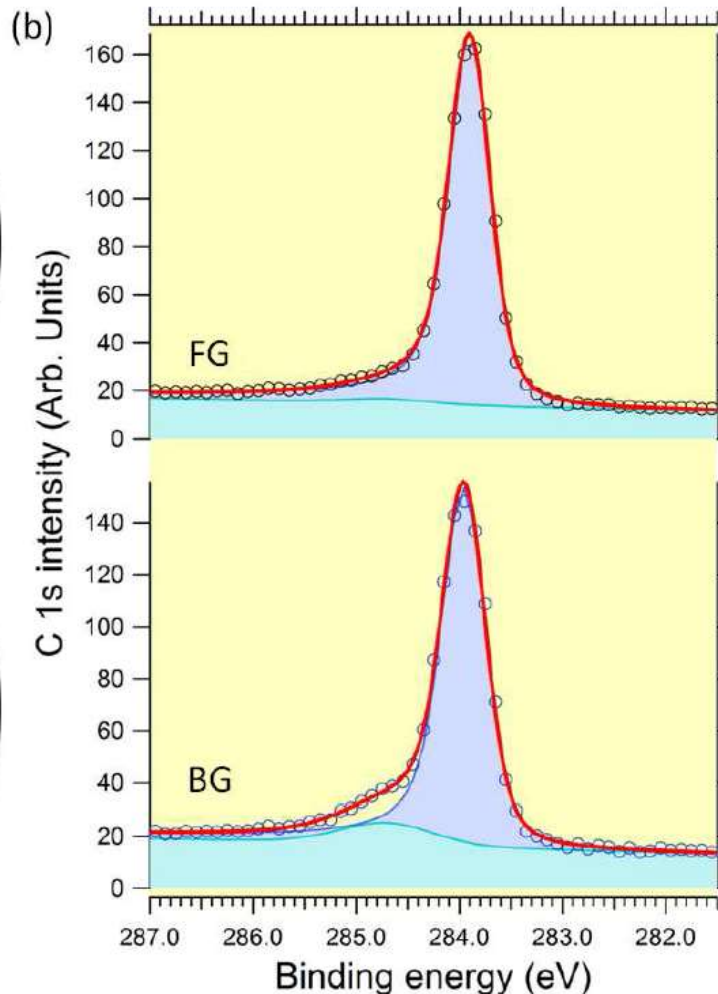
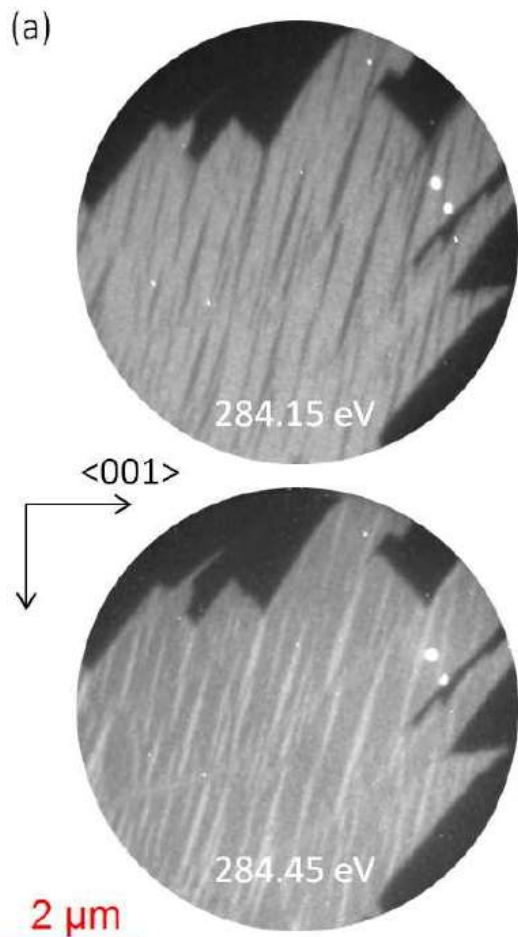
Buckled graphene unit cell by ab-initio



Elettra Sincrotrone Trieste

buckled graphene unit cell

Buckled Graphene



Exceptionally large buckling

GGA:

- ❖ Min Ir-C distance of 1.9 Å
- ❖ Max Ir-C distance of 4.0 Å

DFT-D:

- ❖ Min Ir-C distance of 2.1 Å
- ❖ Max Ir-C distance of 3.7 Å
- ❖ 18 atoms over 160 (i.e. 11%) are **chemisorbed**, the others are physisorbed

Buckled graphene shows regular one-dimensional ripples with periodicity of 2.1nm.

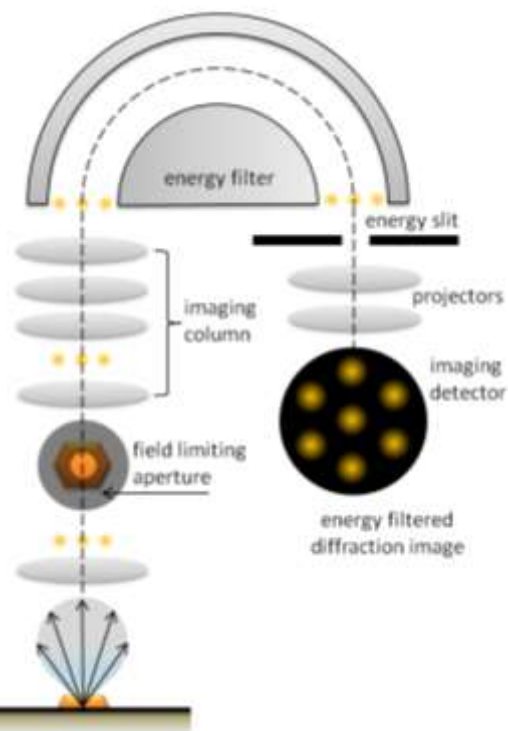
Electronic structure: graphene doping



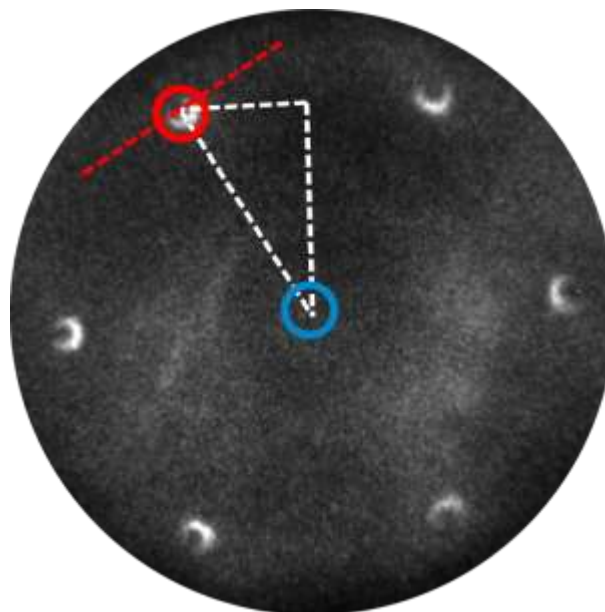
Elettra Sincrotrone Trieste

what is the difference in electronic structure between FG and BG?
do they both show the same Dirac-like dispersion?

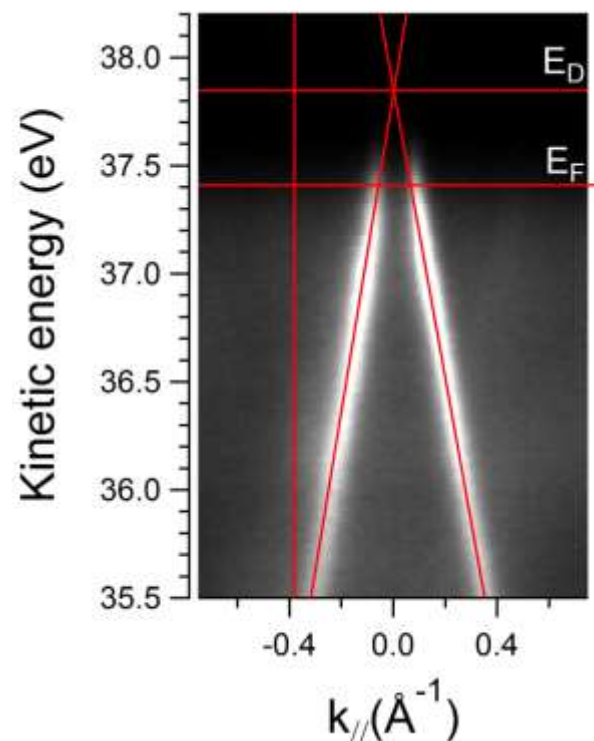
Diffraction Imaging



measurements limited to
2 μm in dia.



μ -ARPES at E_F



$E_D = 0.42 \text{ eV}$

Different character of FG and BG

dark-field

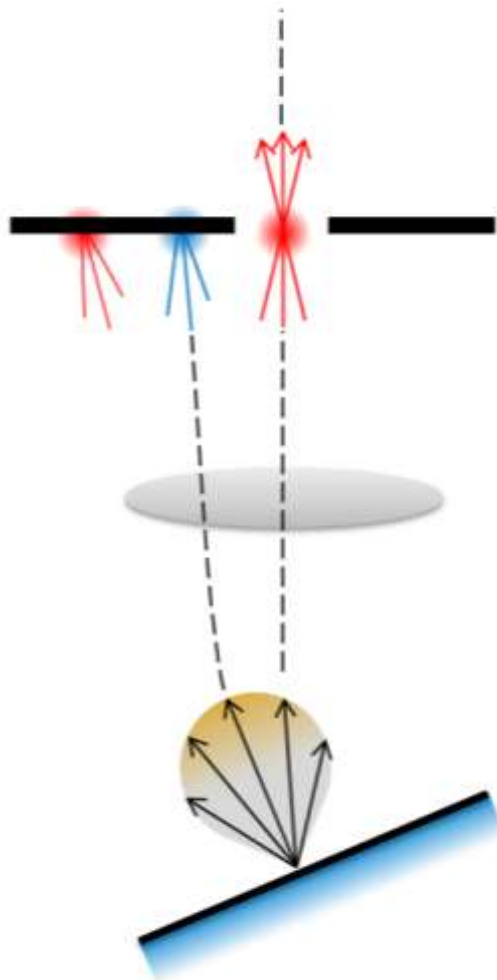
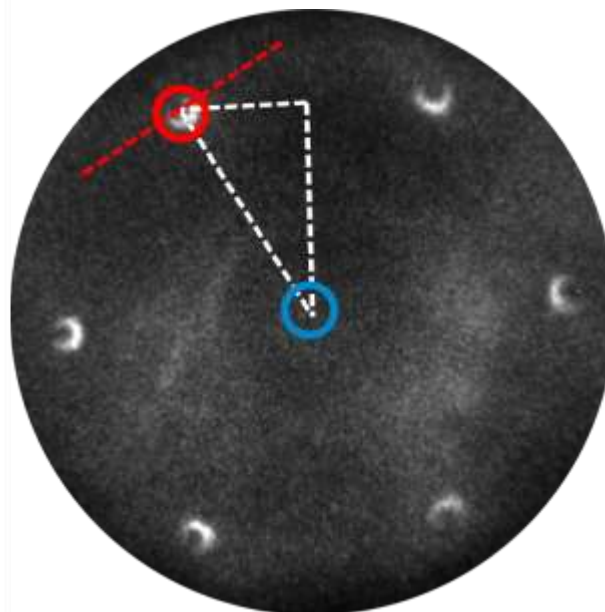
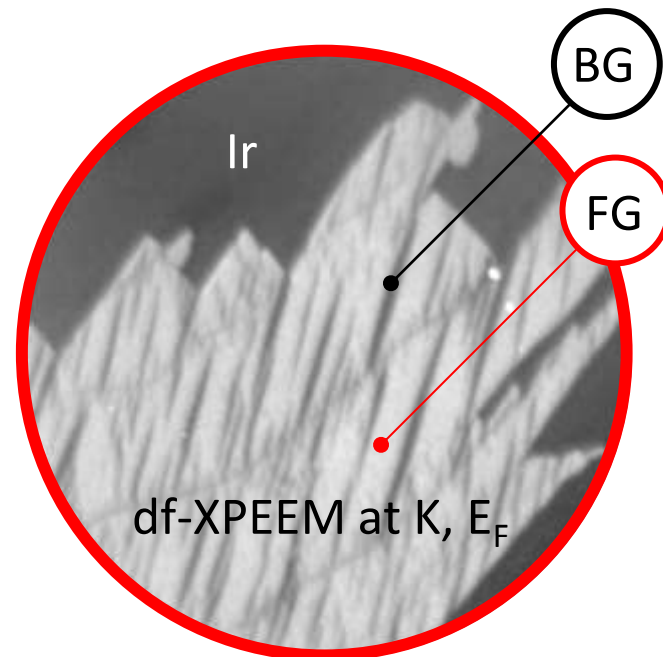


Image intensity proportional to local DOS!



μ -ARPES at E_F



$2 \mu\text{m}$

FG: high DOS at K \rightarrow Dirac cones intact
BG hybridized, metallic-like DOS

Decoupling graphene from substrate:

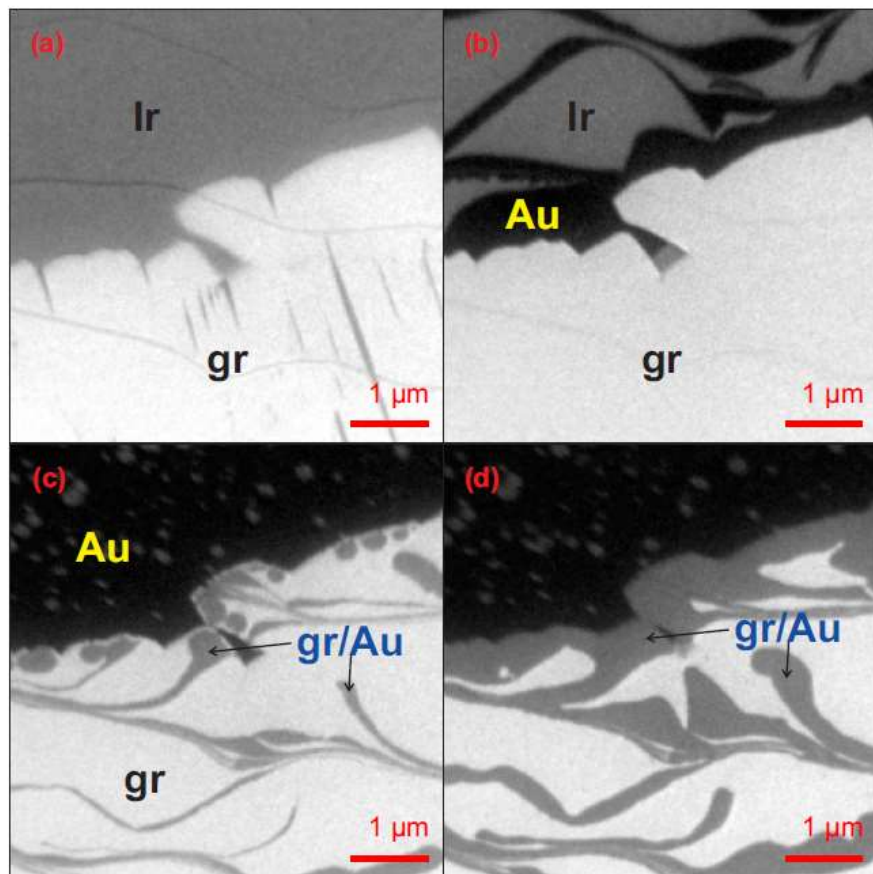
- **Intercalated Au/g/Ir(100)**
- **Switchable formation of carbides in g/Ni(111)**

Tuning the interaction by Au intercalation



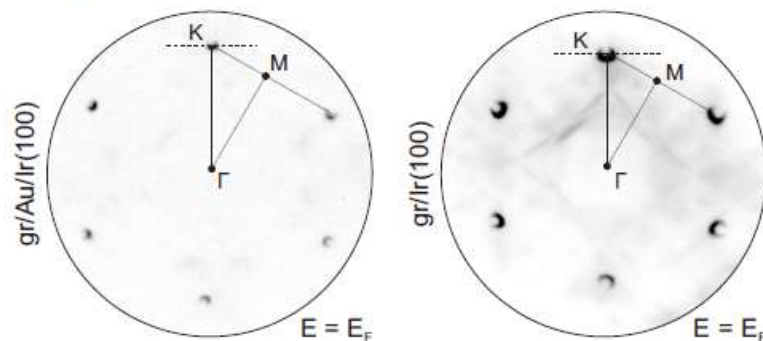
Elettra Sincrotrone Trieste

Real time LEEM imaging during Au intercalation at 600 °C

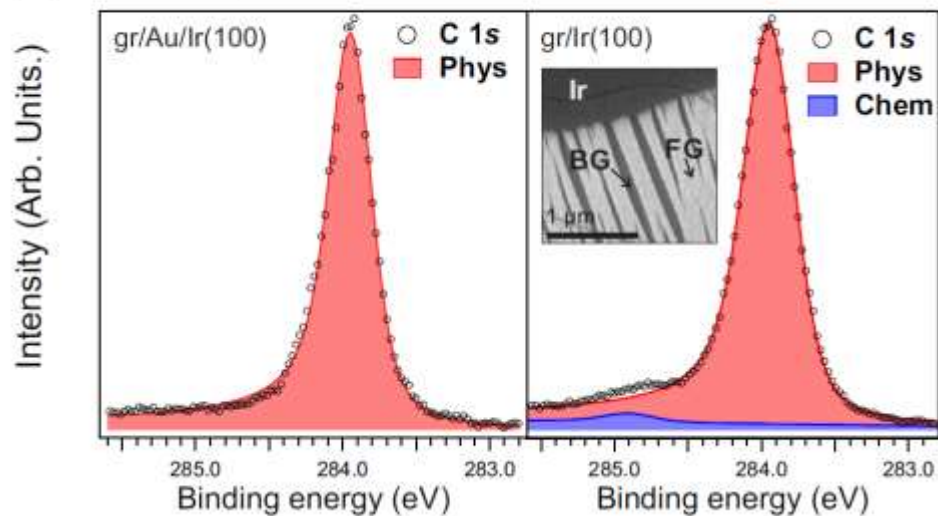


Electronic structure by microprobe ARPES

(a) ARPES



(c) Core level photoemission



Identifying crystal grains in graphene/Ni(111)

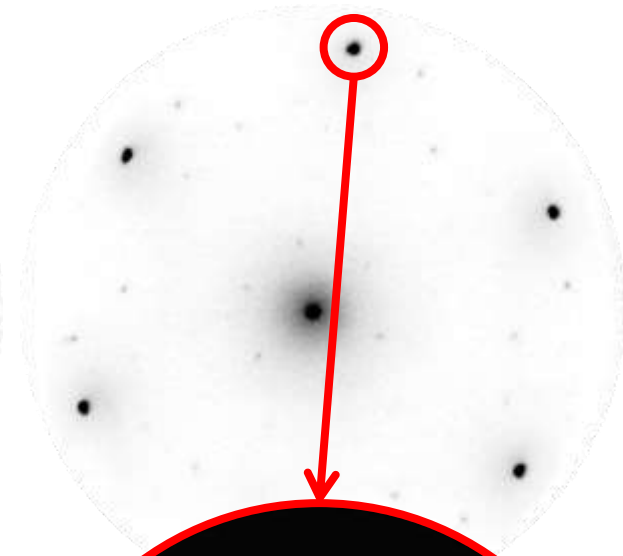
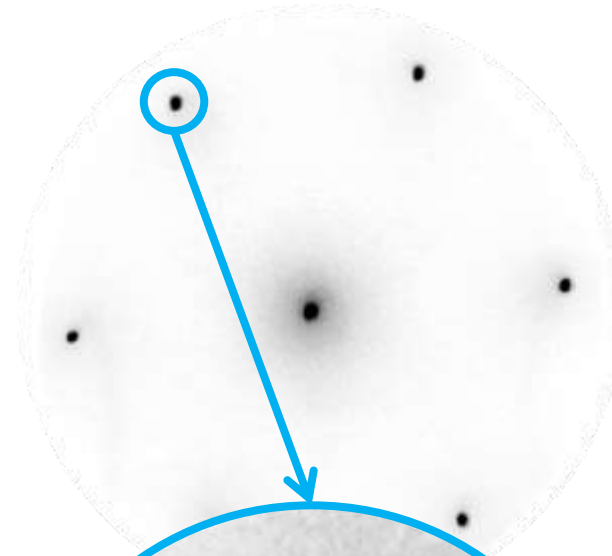
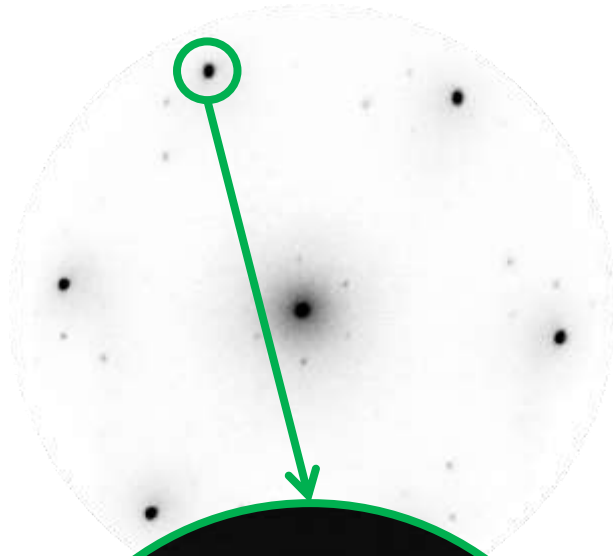


Elettra Sincrotrone Trieste

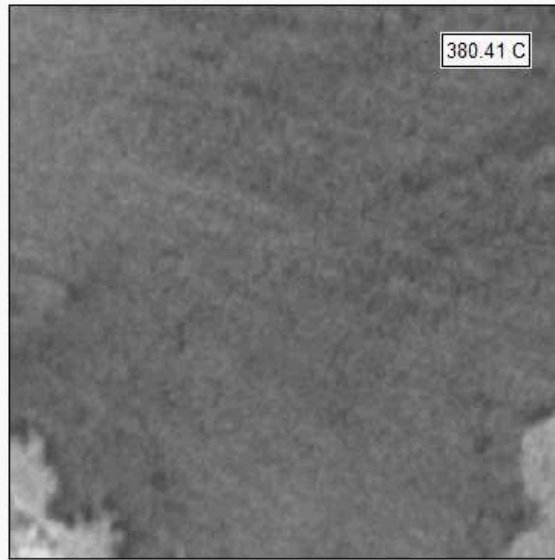
rotated graphene (+17)

epitaxial graphene

rotated graphene (-17)



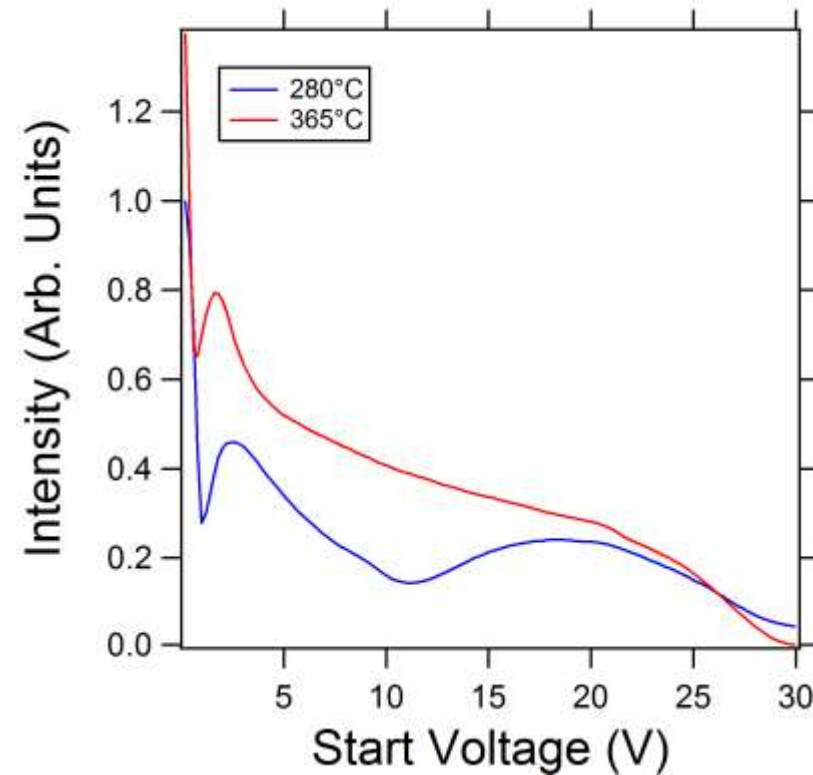
1: carbide nucleation



1 μm

The Ni-carbide nucleates exclusively under rotated graphene, starting at temperatures below 340°C

Different electron reflectivity explains change of contrast

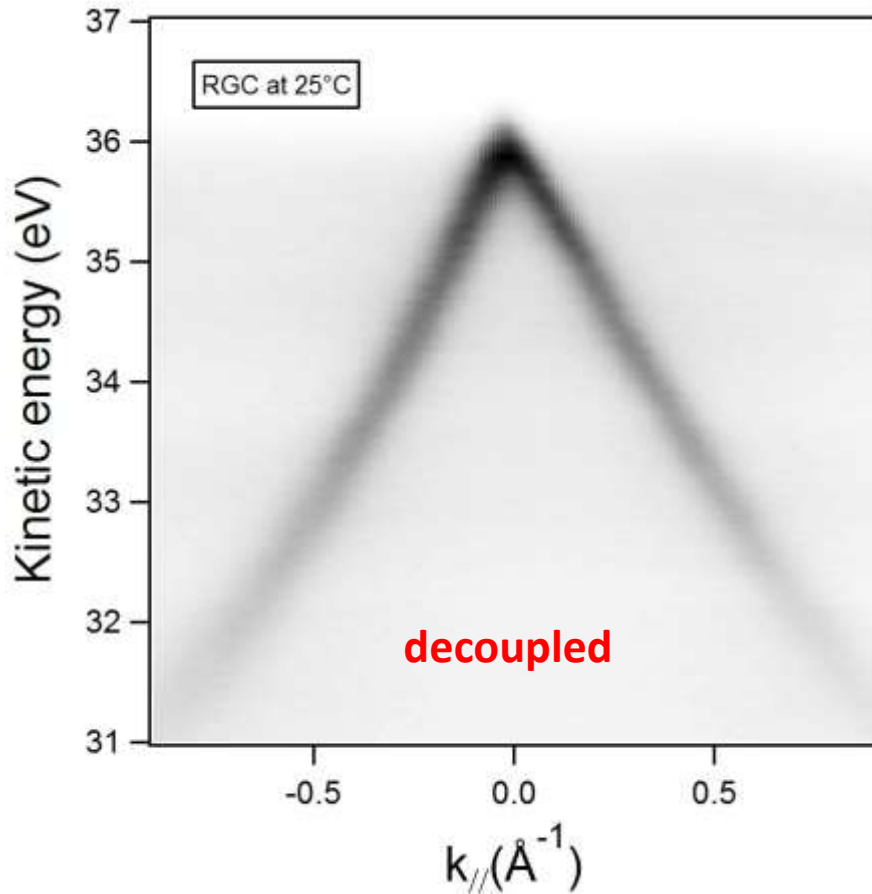


All movies: LEEM FoV 6 μm , electron energy: 11 eV

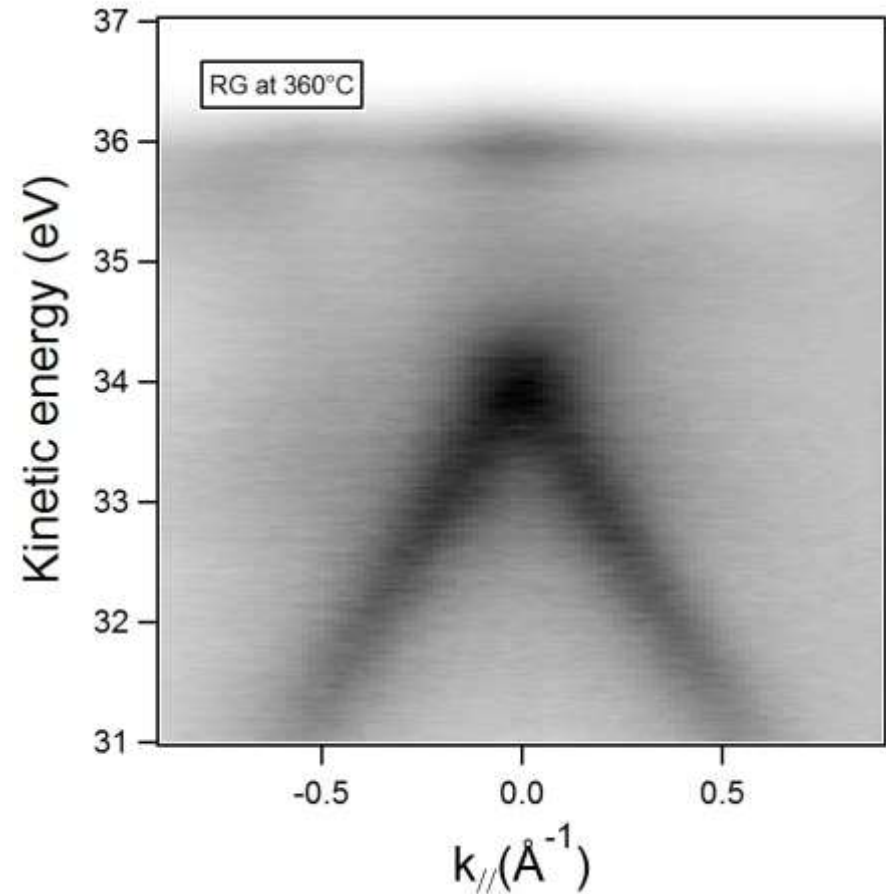
Coupling-decoupling is revealed by μ -ARPES



Elettra Sincrotrone Trieste

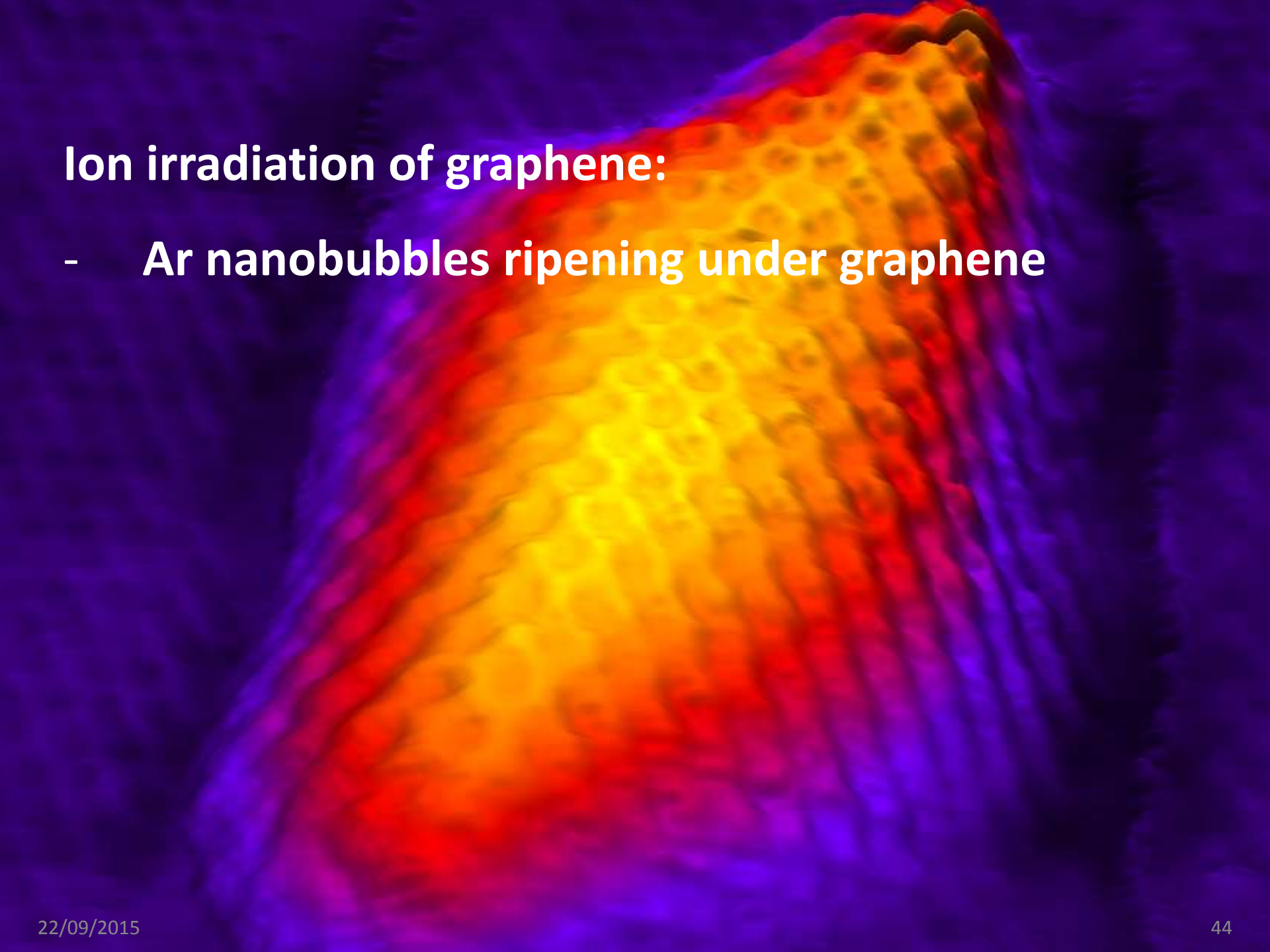


Rotated graphene with Ni-carbide underneath at room temperature;
There's no double layer



Rotated graphene without Ni-carbide underneath at 365°C

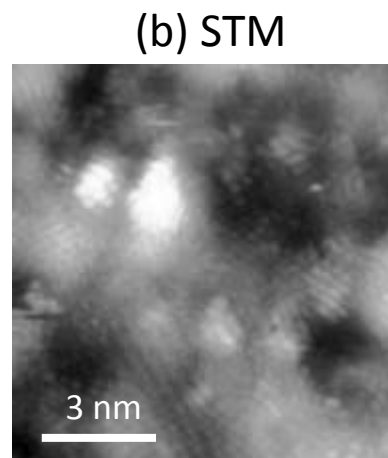
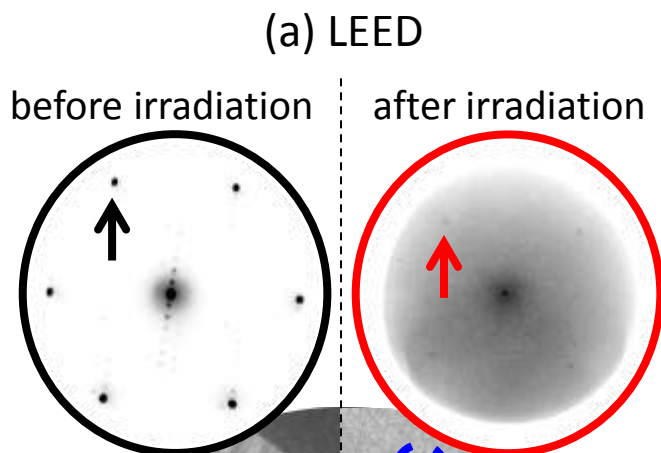
See poster P113 Patera *et al.*



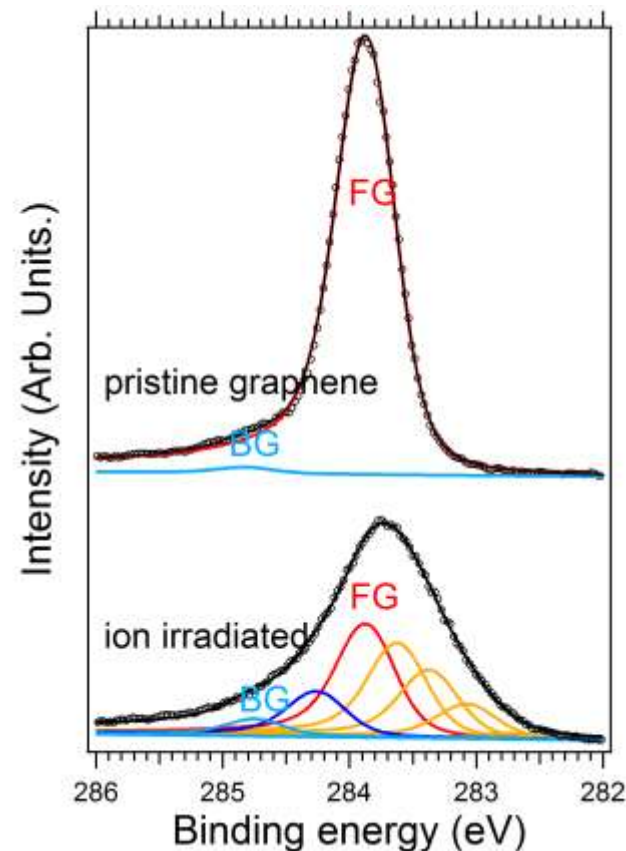
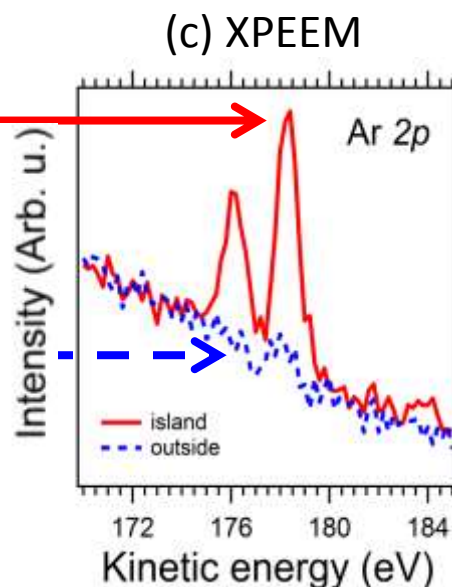
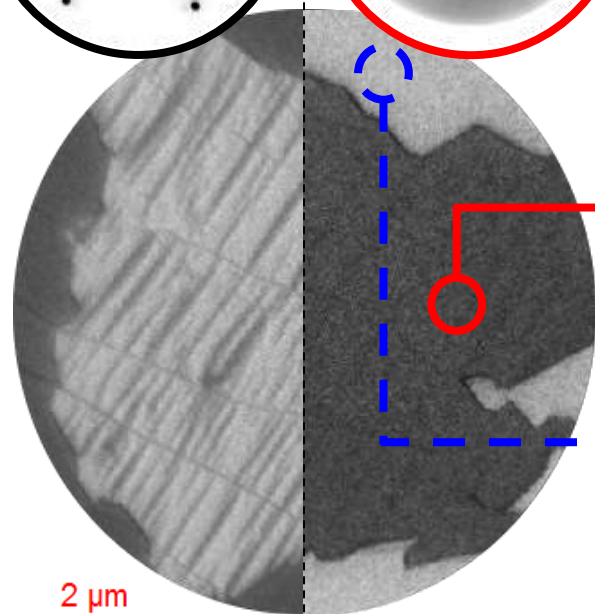
Ion irradiation of graphene:

- **Ar nanobubbles ripening under graphene**

Morphology of Ar⁺ irradiated graphene/Ir(100)



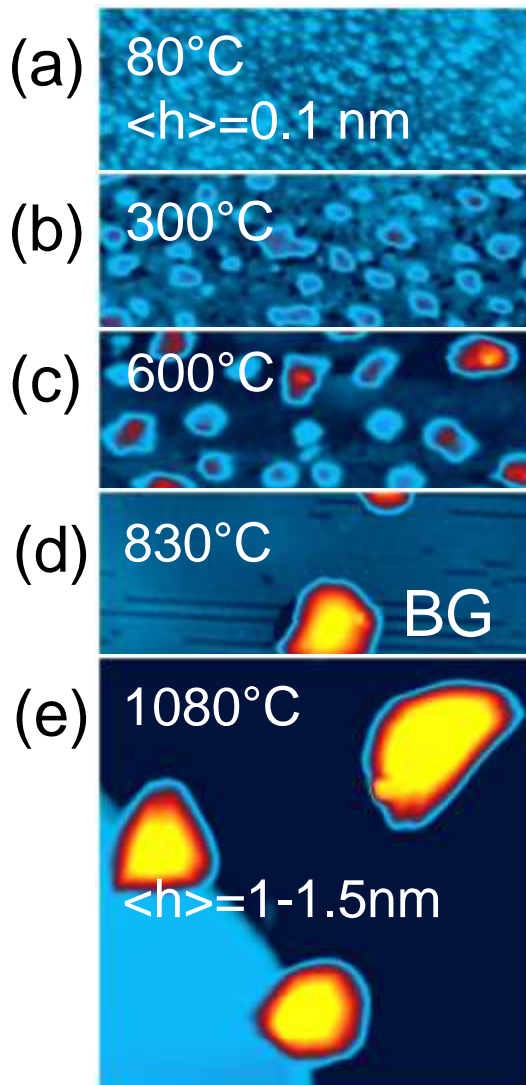
Rough morphology, but ...
graphene is continuous
average height 0.15 nm!



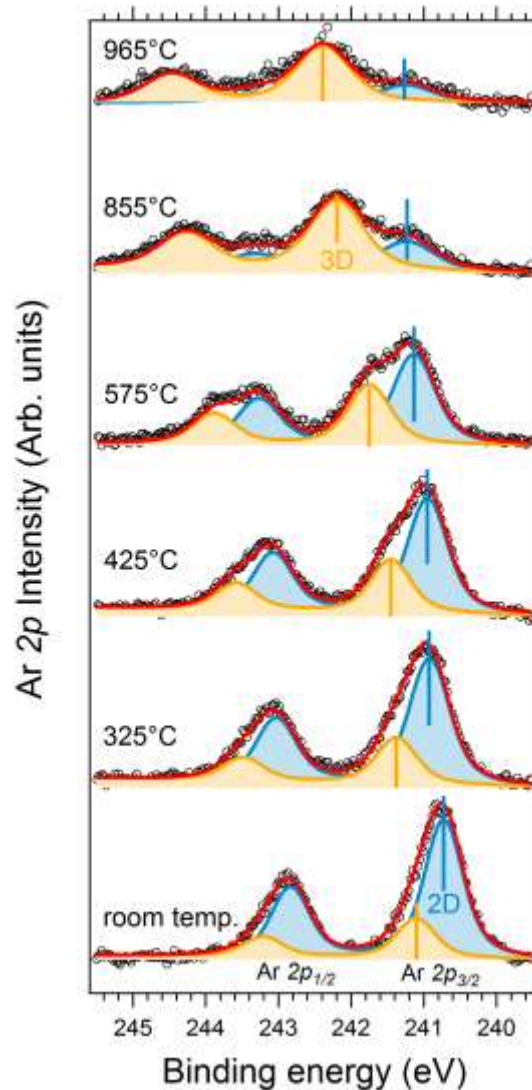
LEEM 12 eV
Irradiation with 0.5keV Ar⁺ 7 s

Evolution upon annealing: STM and μ -XPS

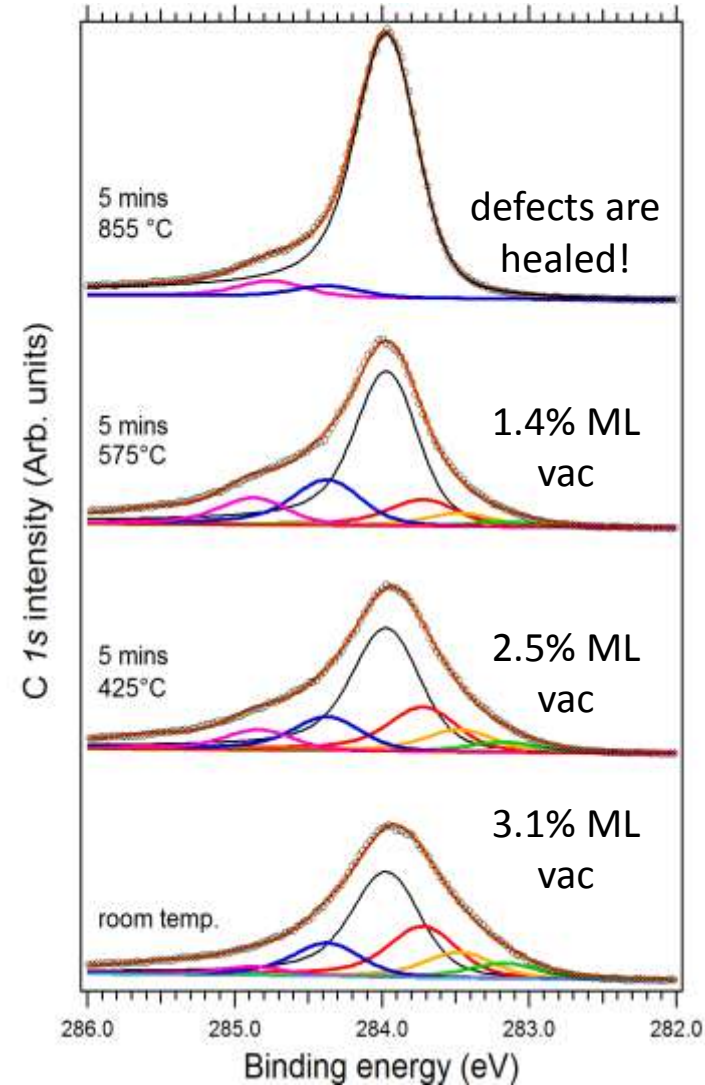
STM



Ar 2p



C 1s

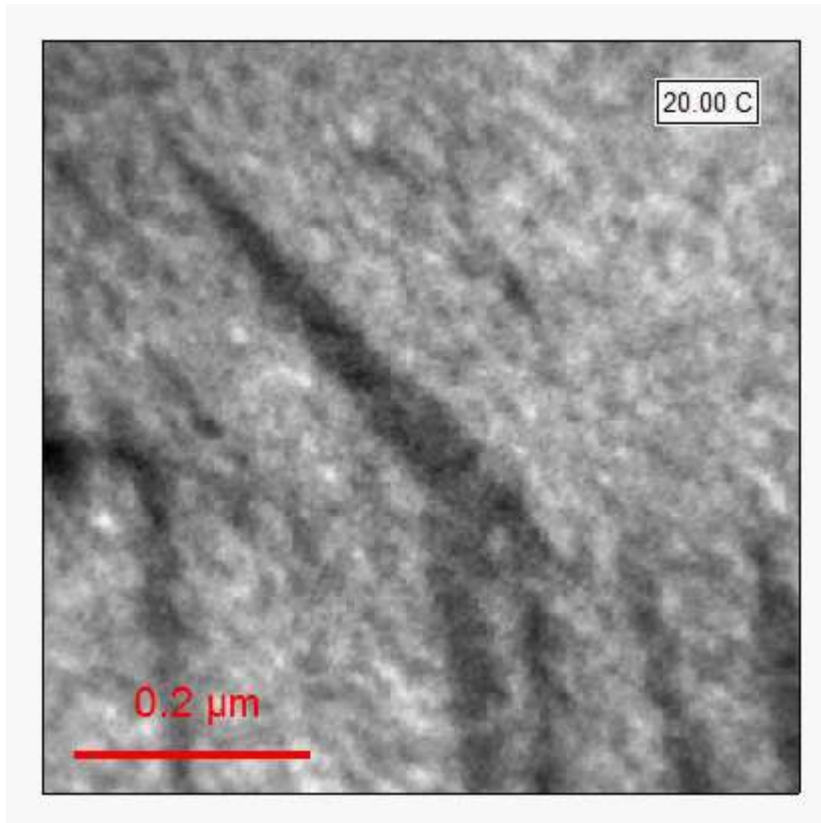


LEEM & XPEEM formation of Ar nanobubbles

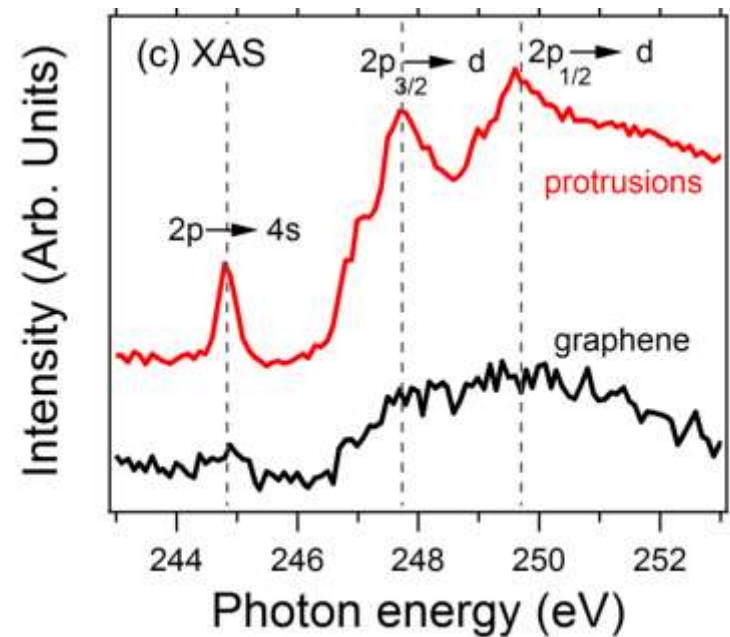
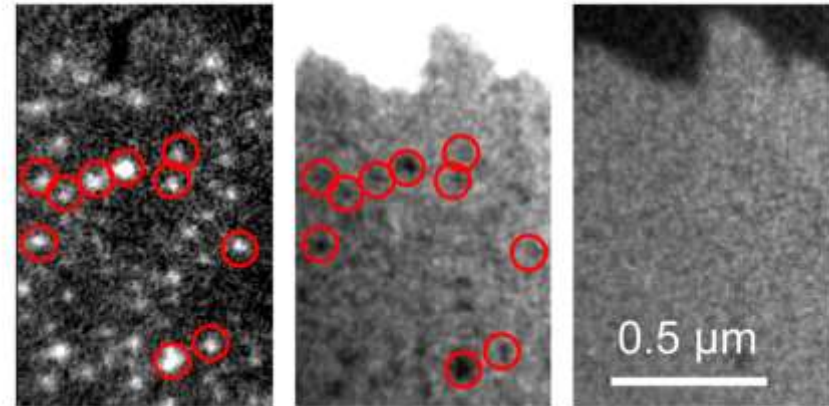


Elettra Sincrotrone Trieste

LEEM movie 12 eV



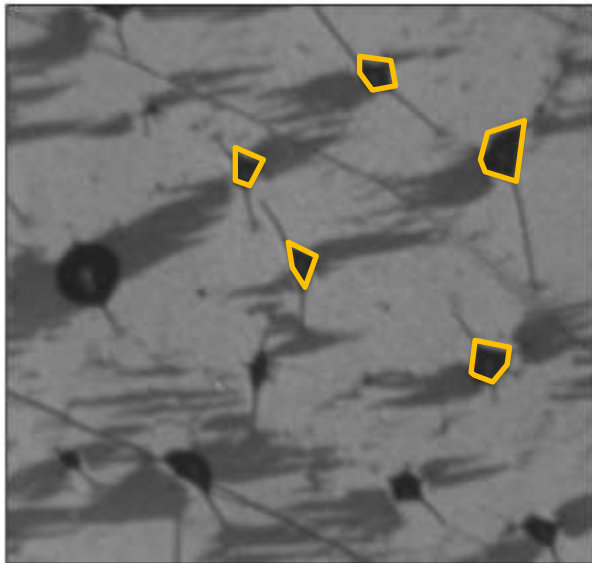
(d) XAS Ar L₃ (e) XPEEM Ir 4f_{7/2} (f) XPEEM C1s



NB formation for g/Ne/Ir(100)

100 eV Ne⁺ ion irradiation was followed by 5 min annealing to 650 °C and subsequent cooling to RT

bright-field LEEM 12 eV



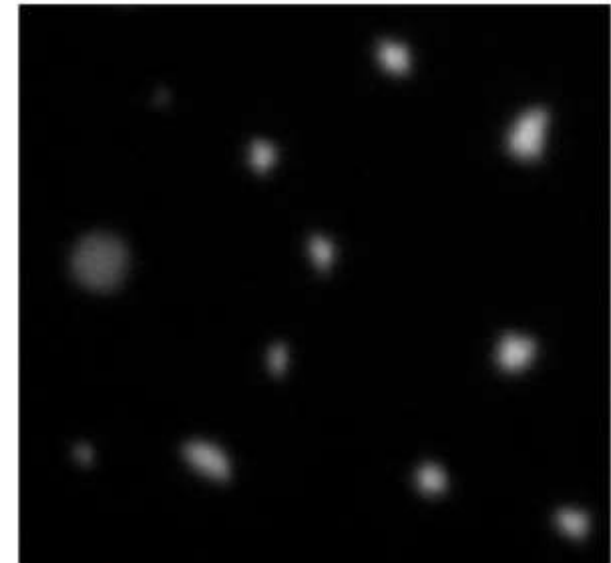
0.5 μm

dark-field LEEM BG phase



0.5 μm

XPEEM imaging Ne 2p



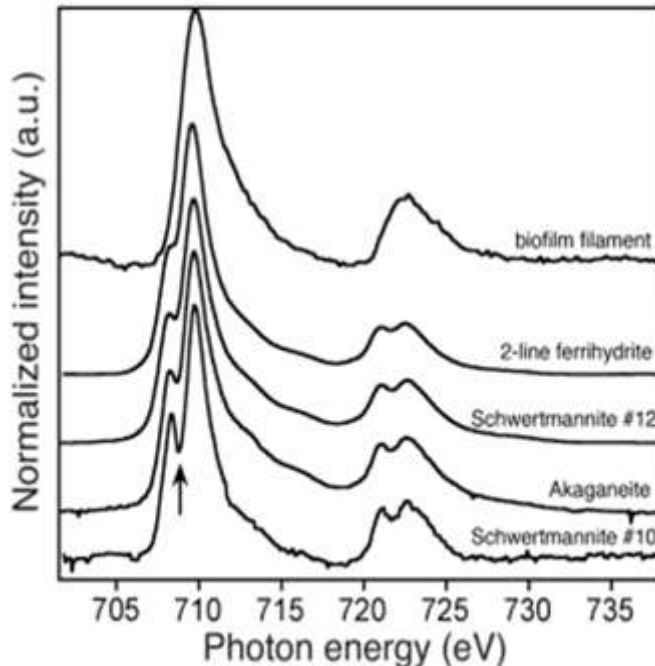
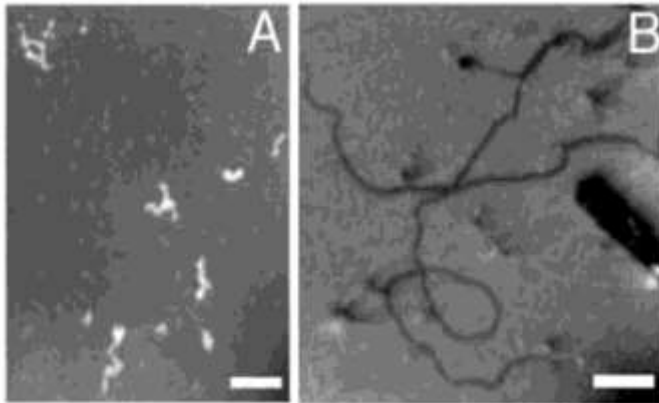
0.5 μm

- Wrinkles surround the larger particles
- At RT, bubbles have a polygonal shape → solid?

- elemental composition below graphene!
- XPS from individual particles
- Shift to high BE for large clusters

XAS-PEEM applications to biosciences

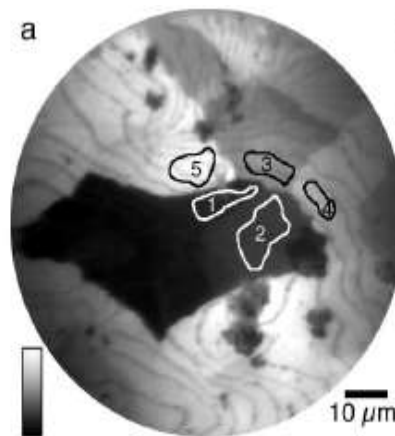
biomineralization



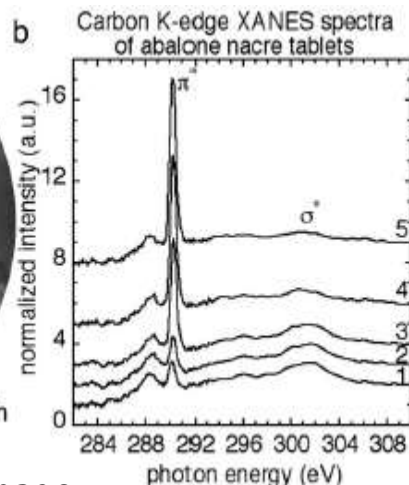
- Bio-mineralization resulting from microbial activity
- X-PEEM images of (A) non mineralized fibrils from the cloudy water above the biofilm (scale bar, 5 μm)
- (B) mineralized filaments and a sheath from the biofilm (scale bar, 1 μm); (bottom)
- X-PEEM Fe L-edge XANES spectra of the FeOOH mineralized looped filament shown in (B), compared with iron oxyhydroxide standards, arranged (bottom to top) in order of decreasing crystallinity.

P.U.P.A Gilbert *et al.* (ALS group),
Science **303** 1656-1658, 2004.

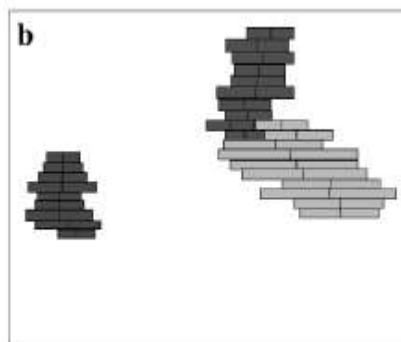
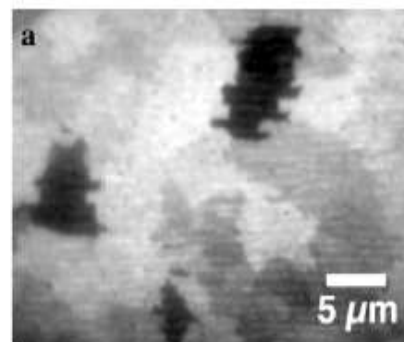
Carbon K-edge image



Carbon K-edge XANES



Oxygen K-edge XAS image



Contrast is observed between adjacent individual nacre tablets, arising because different tablets have different crystal orientations with respect to the radiation's polarization vector.

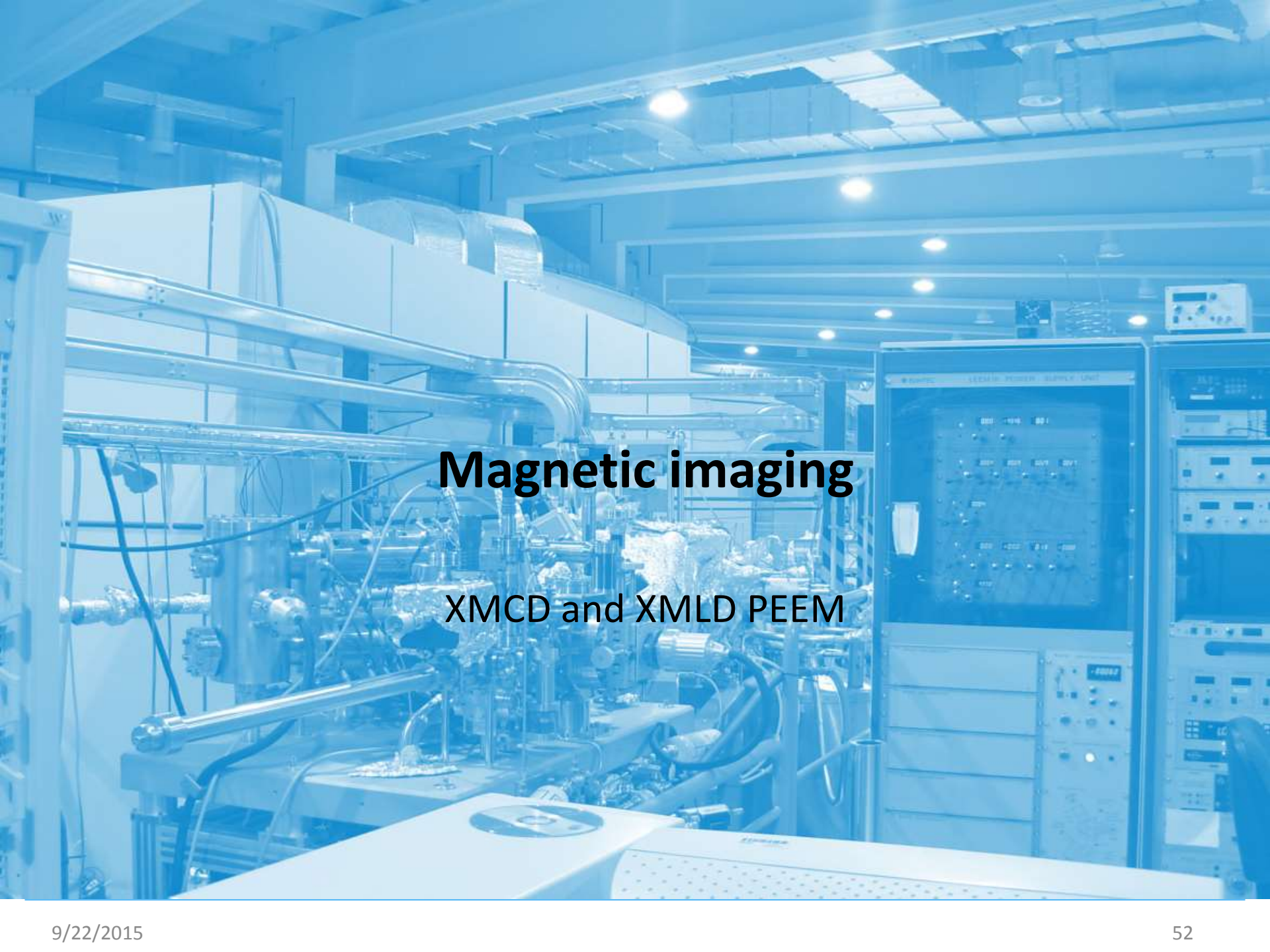
The 290.3 eV peak corresponds to the $C 1s \rightarrow \pi^*$ transition of the CO bond.

Synchrotron radiation is linearly polarized in the orbit plane. Under such illumination, the

intensity of the peak depends on the crystallographic orientation of each nacre tablet with respect to the polarization. This was the first observation of x-ray linear dichroism in a bio-mineral.

$$I(\vartheta, \theta, T) = a + b(3 \cos^2 \vartheta - 1) \langle Q_{zz} \rangle + c(3 \cos^2 \theta - 1) \langle M^2 \rangle_T + d \sum_{i,j} \langle \hat{s}_i \cdot \hat{s}_j \rangle_T$$

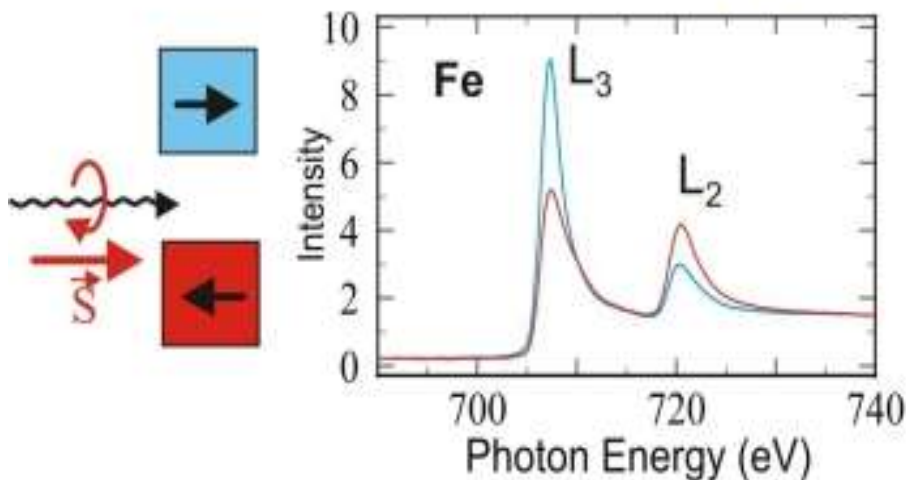
R.A. Metzler *et al.*, *Phys.Rev.Lett.* **98**, 268102 (2007)



Magnetic imaging

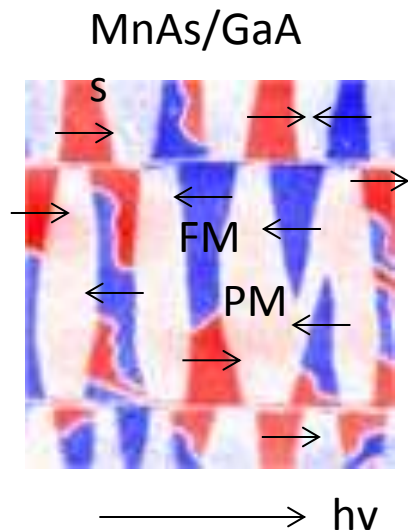
XMCD and XMLD PEEM

Circular Dichroism - Ferromagnets



X-ray magnetic circular dichroism (XMCD) is the dependence of x-ray absorption on the relative orientation of the local magnetization and the polarization vector of the circularly polarized light

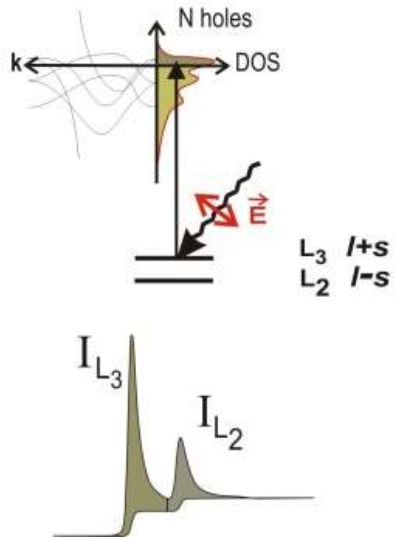
- ✓ Element sensitive technique
- ✓ Secondary imaging with PEEM determine large probing depth (10 nm), buried interfaces.



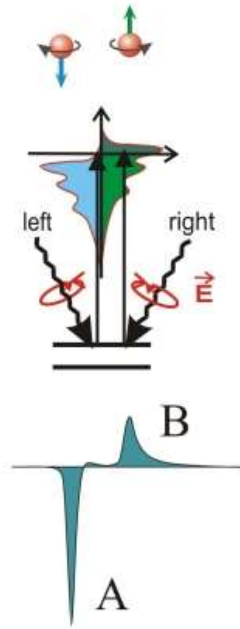
Magnetic domain imaging

At resonance, the secondary electron yield is proportional to the dot product between the magnetization direction and the photon helicity vector, which is parallel or anti-parallel to the beam propagation direction

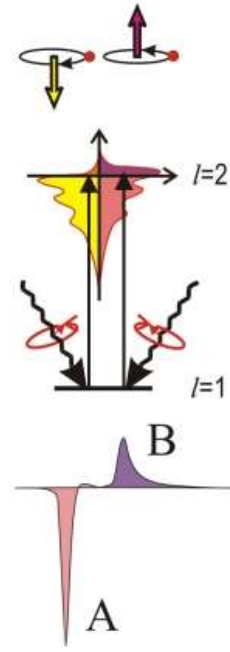
(a) d-Orbital Occupation



(b) Spin Moment



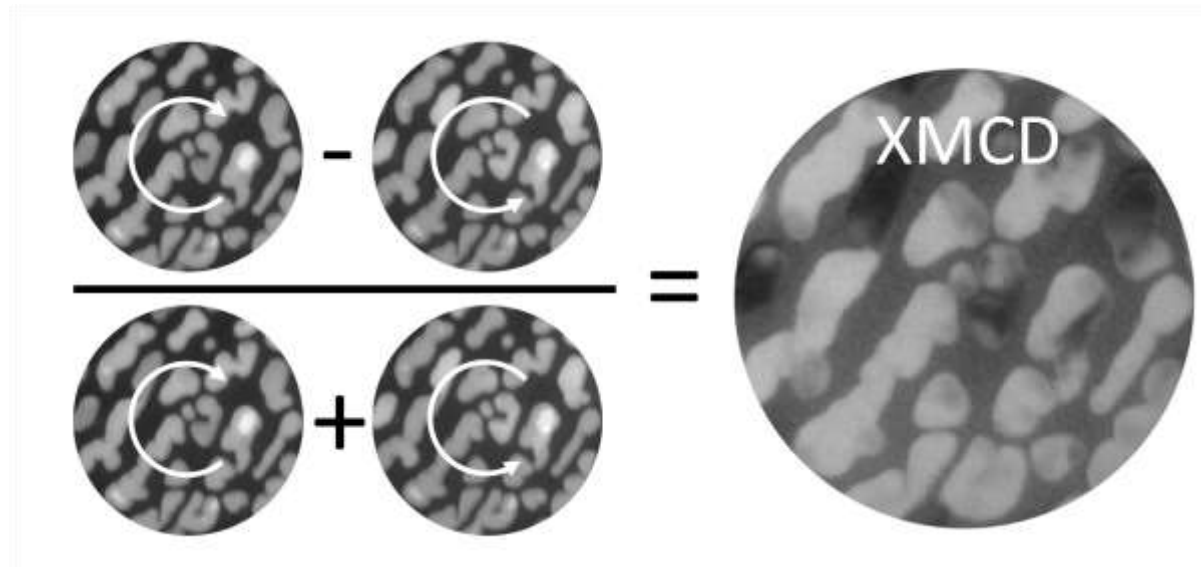
(c) Orbital Moment



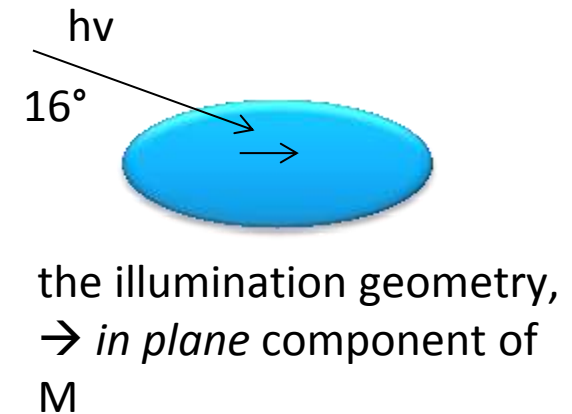
- We **PROBE** 3d elements by exciting 2p into unfilled 3d states
- Dominant channel: $2p \rightarrow 3d$
- White line intensity of the L3 and L2 resonances with the number N of empty d states (holes).

- By using circularly polarized radiation, the angular momentum of the photon can be transferred in part to the spin through the spin-orbit coupling. Photoelectrons with opposite spins are created in the cases of left and right handed polarization. Spin polarization is opposite also for $p_{3/2}$ (L_3) and $p_{1/2}$ (L_2) levels.
- The spin-split valence shell is thus a detector for the spin of the excited photoelectron. The size of the dichroism effect scales like $\cos\theta$, where θ is the angle between the photon spin and the magnetization direction.
- **Refs: IBM. J. Res. Develop. 42, 73 (1998) and J. Magn. Magn. Mater. 200, 470 (1999).**

The size of the dichroism effect scales like $\cos\theta$, where θ is the angle between the photon spin and the magnetization direction. Hence the maximum dichroism effect (typically 20%) is observed if the photon spin and the magnetization directions are parallel and anti-parallel. Sum rules allows measuring orbital and spin moments

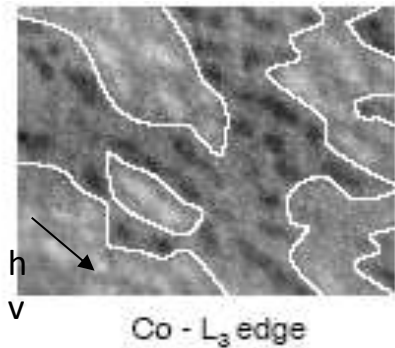


Geometry



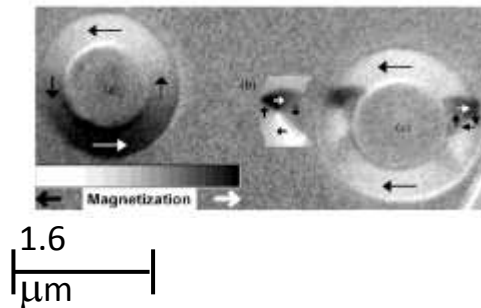
MAGNETIC STATE using XMCD & XMLD

Co nanodots on Si-Ge

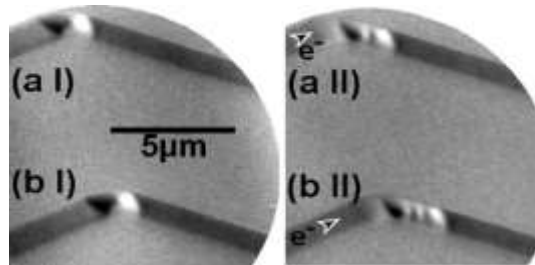


A. Mulders et al,
Phys. Rev. B 71,
214422 (2005).

patterned structures

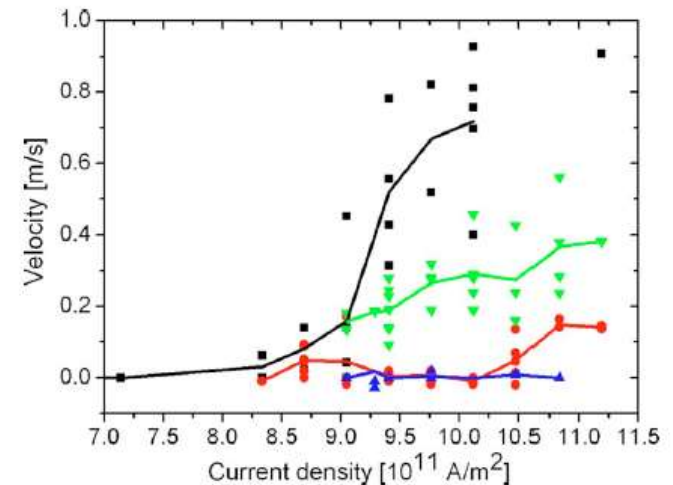


pulse injection



M. Klauui et al,
PRL, PRB 2003 - 2010

domain wall motion induced by spin currents



Laufenberg et al,
APL 88, 232507(2006).

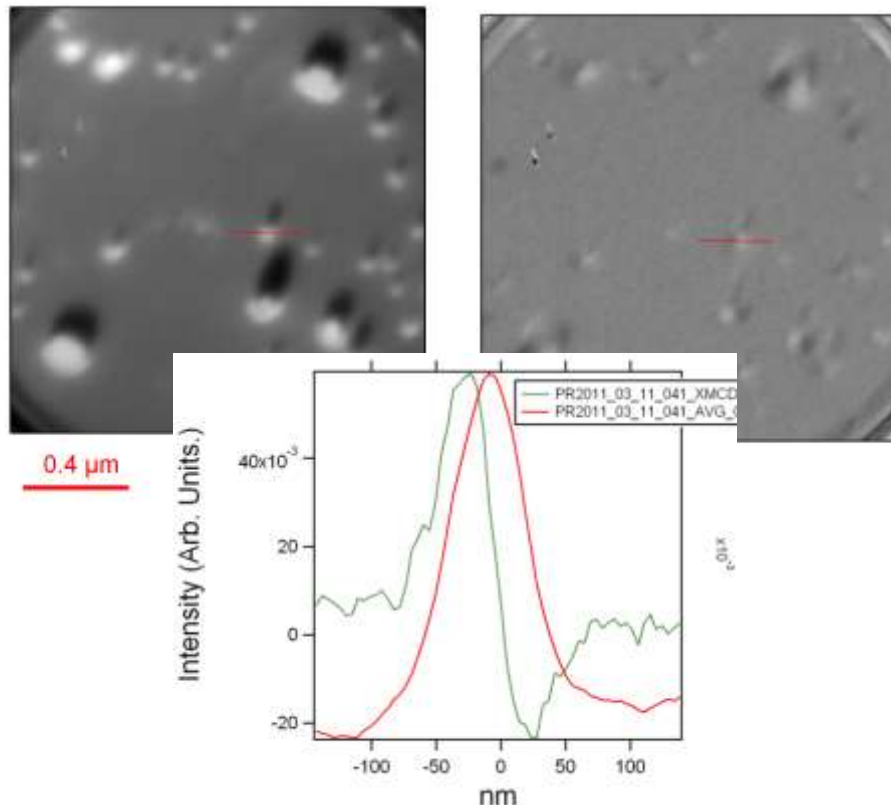
Examples of XMCD-PEEM applications



Elettra Sincrotrone Trieste

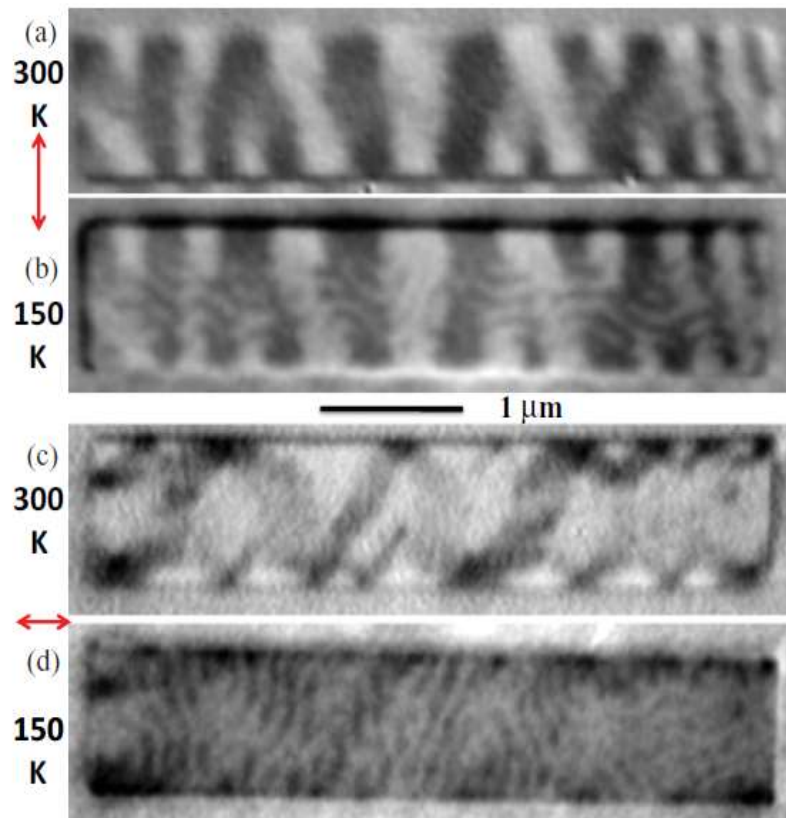
nano-magnetism of (Ga,Fe)N films

Fe L3 edge (chemical) Fe L3 edge (XMCD)



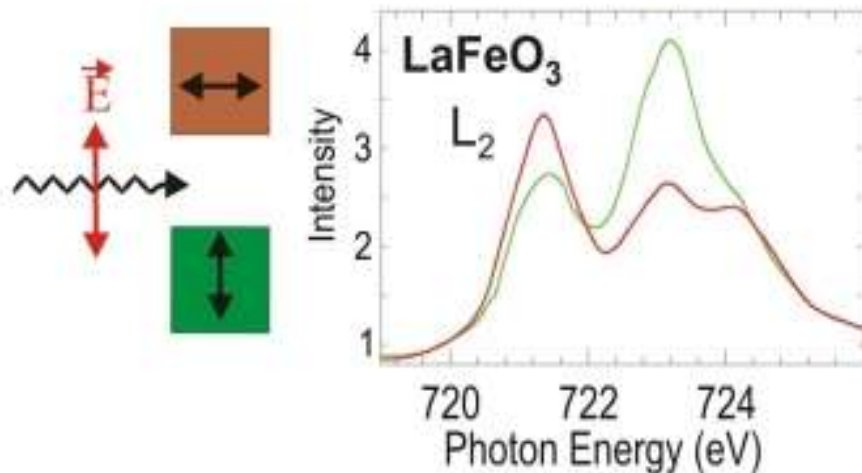
I Kowalik, D. Arvanitis, M.A. Niño et al.,
in preparation

Magnetization in NiPd nanostructures



J.-Y. Chauleau, Phys. Rev. B 84, 094416
(2011)

Linear Dichroism - Antiferromagnets



In the presence of spin order the spin-orbit coupling leads to preferential charge order relative to the spin direction, which is exploited to determine the spin axis in antiferromagnetic systems.

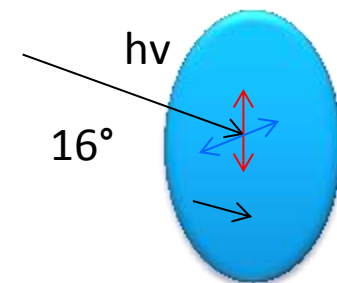
- ✓ Element sensitive technique
- ✓ Secondary imaging with PEEM determine large probing depth (10 nm), buried interfaces.
- ✓ Applied in AFM systems (oxides such as NiO)

Absorption intensity at resonance

$$I(\vartheta, \theta, T) = a + b(3 \cos^2 \vartheta - 1) \langle Q_{zz} \rangle + c(3 \cos^2 \theta - 1) \langle M^2 \rangle_T + d \sum_{i,j} \langle \hat{s}_i \cdot \hat{s}_j \rangle_T$$

1st term: quadrupole moment, i.e. electronic charge (not magnetic!)

2nd term determines XMLD effect; θ is the angle between E and magnetic axis A; XMLD max for E || A;



Linear vertical and linear horizontal polarization of the photon beam

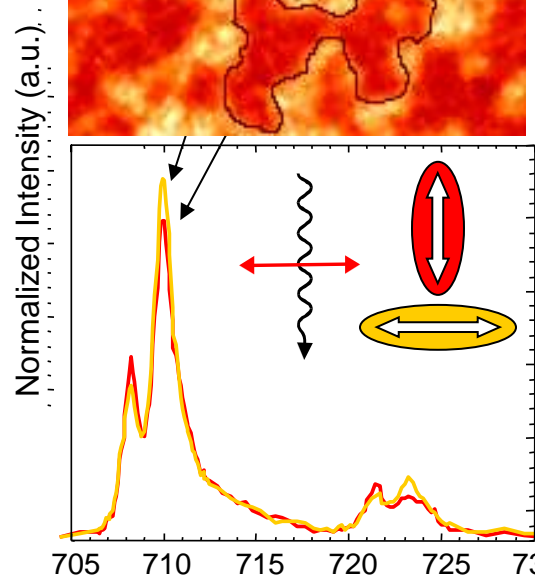
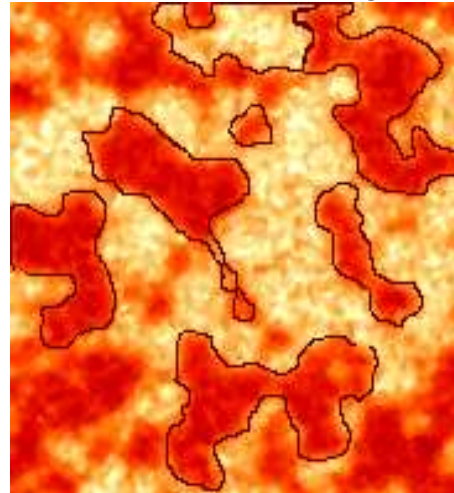
Direct observation of the alignment of ferromagnetic spins by antiferromagnetic spins

F. Nolting⁺, A. Scholl⁺, J. Stöhr[†], J. W. Seo^{‡§}, J. Fompeyrine[§], H. Siegwart[§], J.-P. Locquet[§], S. Anders⁺, J. Lüning[†], E. E. Fullerton[†], M. F. Toney[†], M. R. Scheinfein^{||} & H. A. Padmore⁺

Nature, 405 (2000), 767.

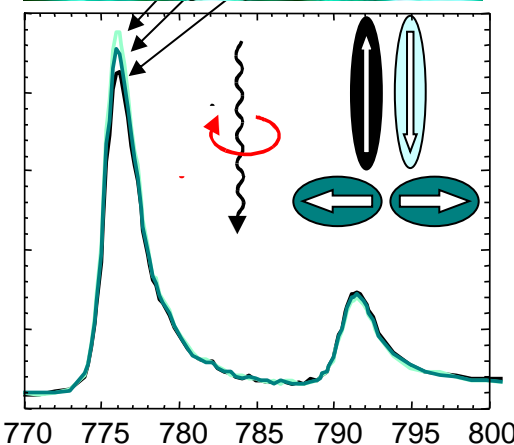
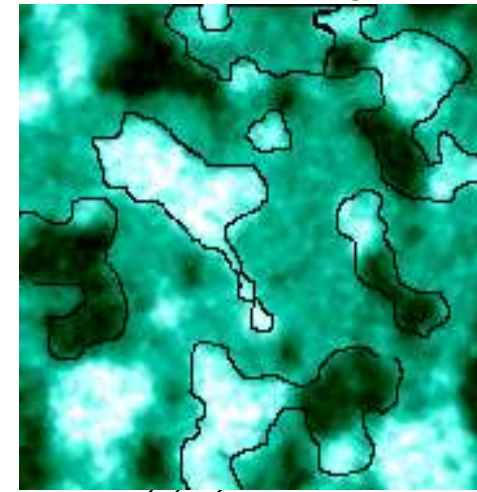
ferromagnet/antiferromagnet
Co/LaFeO₃ bilayer
interface exchange coupling
between the two materials

LaFeO₃ layer
XMLD Fe L₃



Photon Energy (eV)

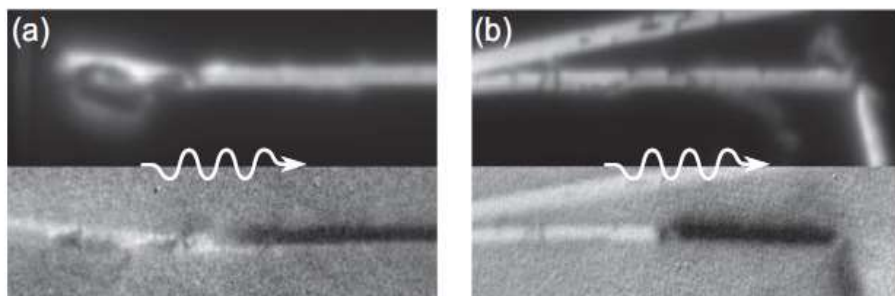
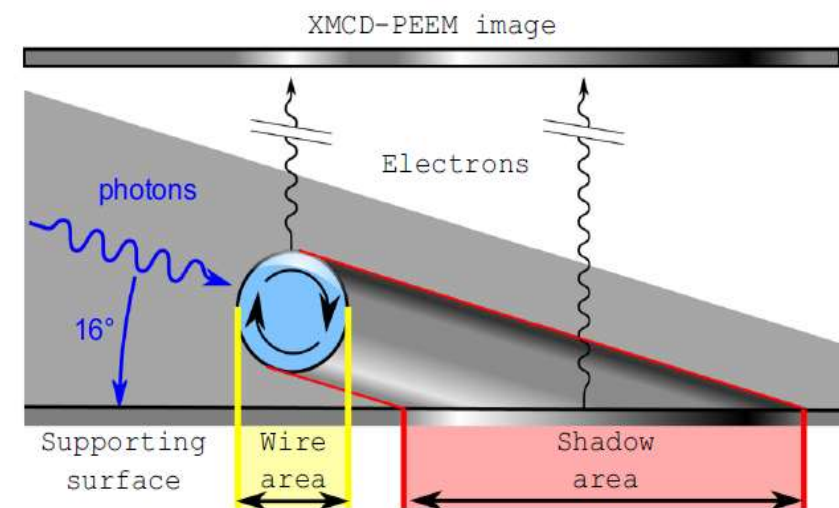
Co layer
XMCD Co L₃/L₂



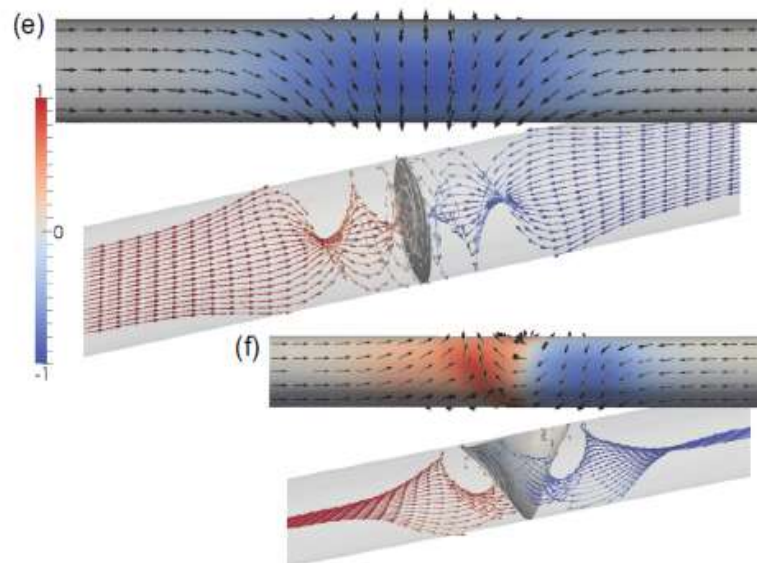
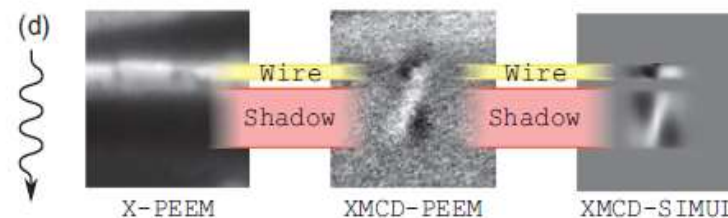
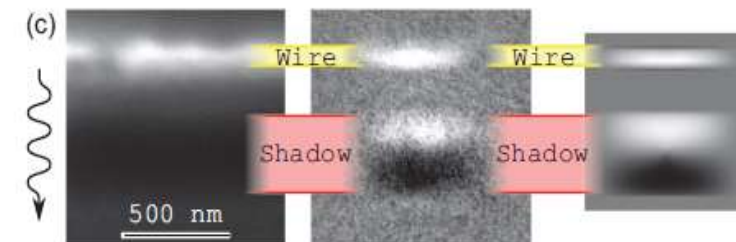
Photon Energy (eV)

DW imaging in magnetic wires

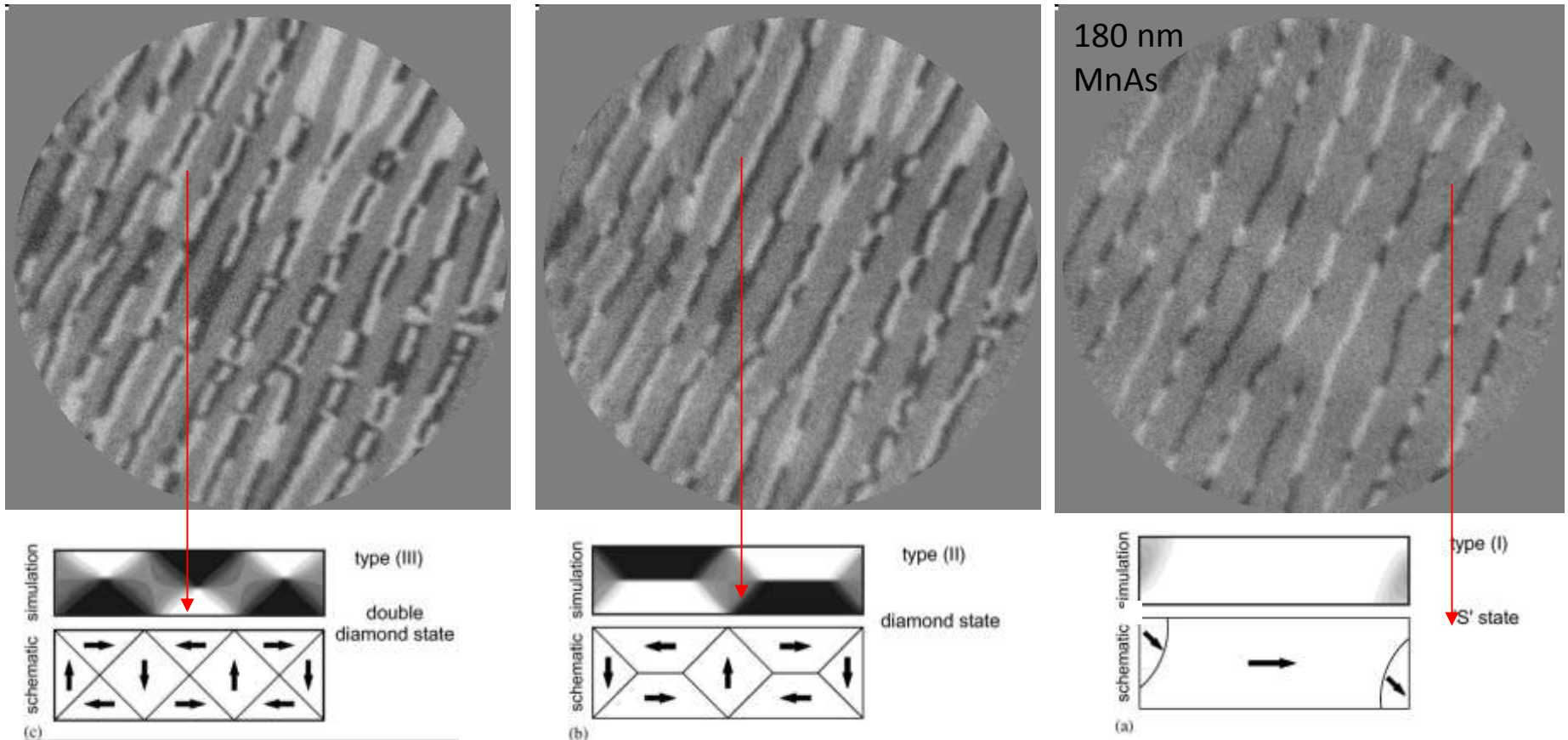
Observation of Bloch-point domain walls in cylindrical magnetic



wire



Experiment: Straight walls; Head to head domains



Simulation: Cross sectional cut: diamond state

R. Engel-Herbert et al, J. Magn. Magn. Mater. 305, (2006) 457



Adding the time domain to PEEM

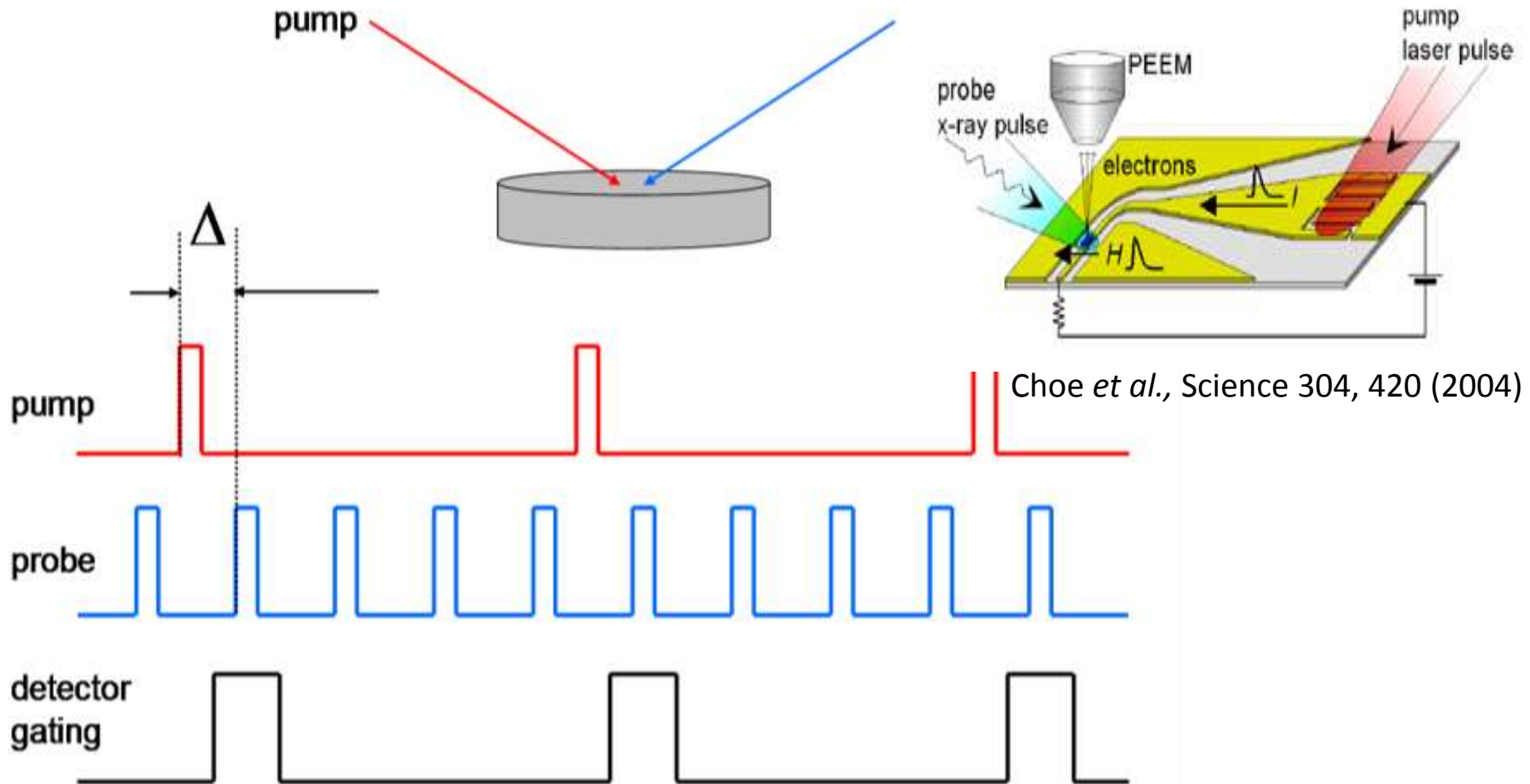
TR-PEEM methods

Time-resolved PEEM: the stroboscopic approach



Elettra Sincrotrone Trieste

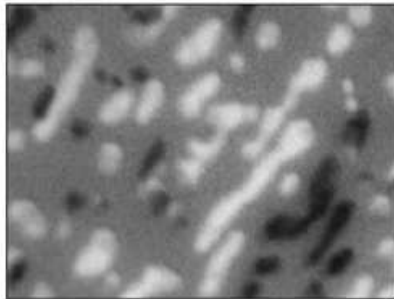
Stroboscopic experiments combine high lateral resolution of PEEM with high time resolution, taking advantage of pulsed nature of synchrotron radiation



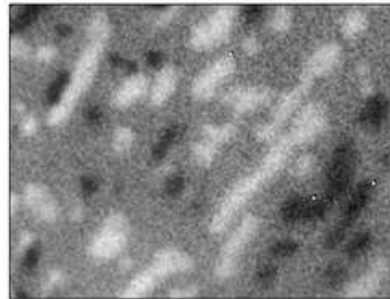
Detector gating for time-resolved XMCD PEEM



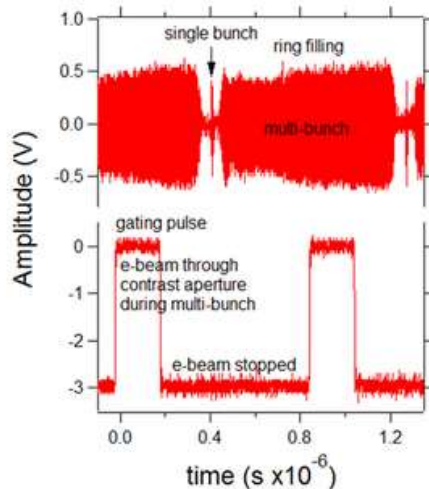
Elettra Sincrotrone Trieste



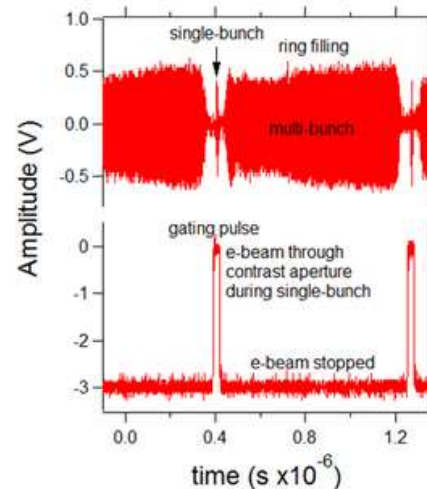
Multi-bunch image
32 images per helicity
Image exposure 4 s
Acquisition time: 5':18"



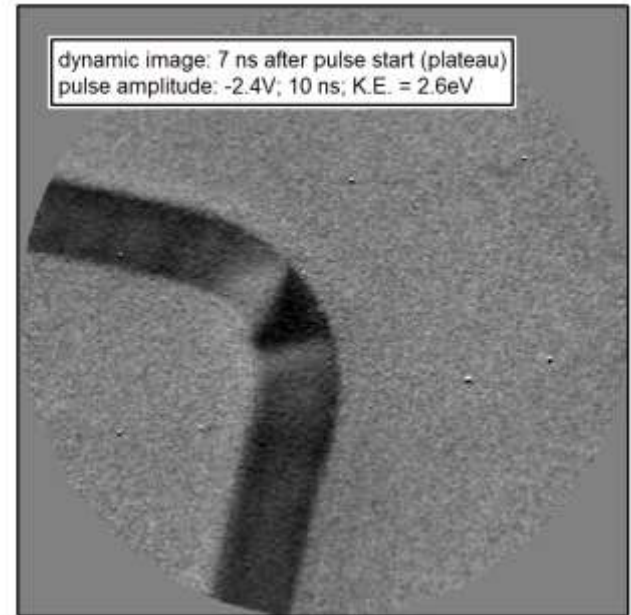
Single bunch image
24 images per helicity
Image exposure 20 s
Acquisition time: 17':40"



pulse width 200 ns



pulse width 30 ns



2 μm

Current-induced motion of magnetic domain walls in Permalloy (Fe₂₀Ni₈₀) nanostripes, through the spin-transfer torque (STT) effect. Our measurements reveal clear eformations of the domain wall shape

- **Switching processes** (magnetisation reversal) in magnetic elements (in spin valves, tunnel junction)
 - Nucleation, DW propagation or both?
 - Effect of surface topography, morphology crystalline structure etc.
 - Domain dynamics in Landau flux closure structures.
- response of vortices, domains, domain walls in Landau closure domains in the **precessional regime**
- **Stroboscopic technique:**
 - only reversible processes can be studied by pump – probe experiments
 - Measurements are quantitative

Quantitative Analysis of Magnetic Excitations in Landau Flux-Closure Structures Using Synchrotron-Radiation Microscopy

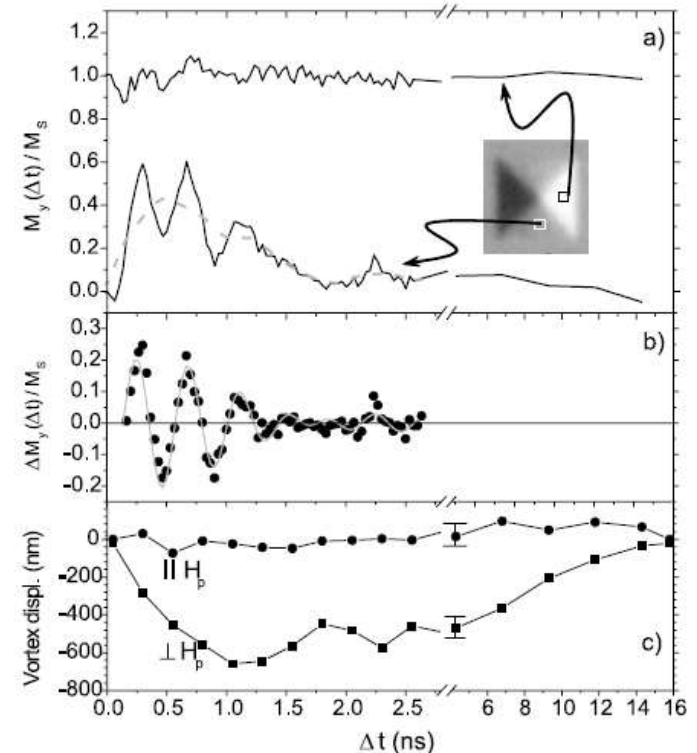
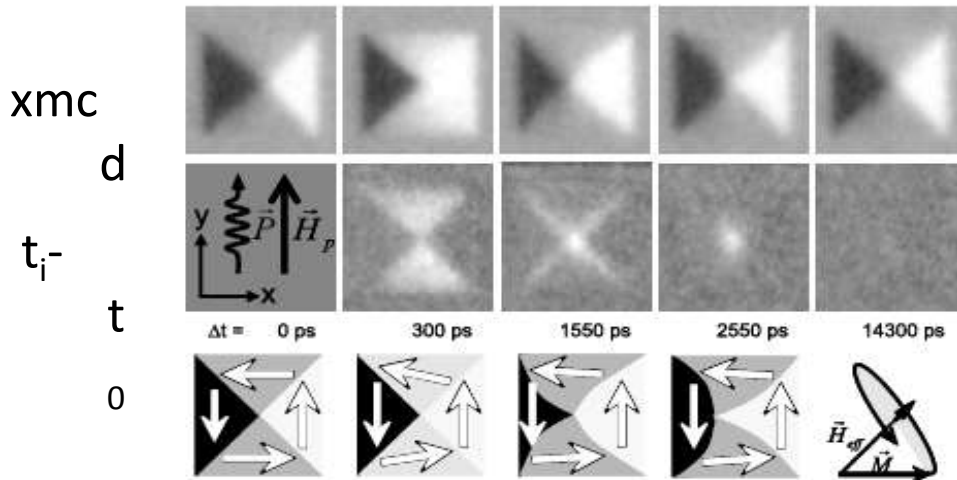
J. Raabe,^{1,*} C. Quitmann,¹ C. H. Back,² F. Nolting,¹ S. Johnson,¹ and C. Buehler¹

The time dependent magnetization is described by the phenomenological Landau-Lifshitz-Gilbert equation

$$\frac{d\vec{M}}{dt} = -\gamma_0 \vec{M} \times \vec{H}_{\text{eff}} + \frac{\alpha}{M} \left(\vec{M} \times \frac{d\vec{M}}{dt} \right).$$

The first term describes the precession of the magnetization \vec{M} about the total effective field \vec{H}_{eff} . The second term describes the relaxation back into the equilibrium state using the dimensionless damping parameter α .

torque $\vec{T} = -\gamma_0 \vec{M} \times \vec{H}_{\text{eff}}$

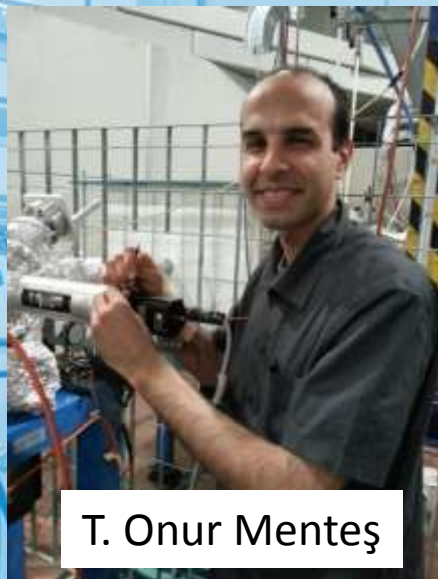


- XPEEM is a versatile full-field imaging technique. Combined with SR it allows us to implement laterally resolved versions of the most popular x-ray spectroscopies taking advantage of high flux of 3rd generation SR light sources.
- In particular, XAS-PEEM combines element sensitivity with chemical sensitivity (e.g. valence), and, more importantly, magnetic sensitivity. Magnetic imaging has been the most successful application of PEEM (next tutorial lecture!).
- XPEEM or energy-filtered PEEM adds true chemical sensitivity to PEEM. Modern instruments allow to combine chemistry with electronic structure using ARUPS.
- XPEEM can be complemented by LEEM, which adds structure sensitivity and capability to monitor dynamic processes.
- Lateral resolution will approach the nm range as AC instruments become available. Limitations due to space charge are not yet clear
- Novel application fields are being approached, such as biology, geology and earth sciences. HAXPES will increase our capabilities to probe buried structures (bulk).

Reviews and topical papers on x-ray spectromicroscopy and XPEEM

- S. Guenther, B. Kaulich, L. Gregoratti, M. Kiskinova, *Prog. Surf. Sci.* **70**, 187–260 (2002).
- E. Bauer, *Ultramicroscopy* **119**, 18–23 (2012).
- E. Bauer, *J. Electron. Spectrosc. Relat. Phenom.* (2012):
<http://dx.doi.org/10.1016/j.elspec.2012.08.001>
- G. Margaritondo, *J. Electron. Spectrosc. Relat. Phenom.* **178–179**, 273–291 (2010) .
- A. Locatelli, E. Bauer, *J. Phys.: Condens. Matter* **20**, 093002 (2008) .
- G. Schönhense *et al.*, in “*Adv. Imaging Electron Phys.*”, vol. **142**, Elsevier, Amsterdam, P. Hawkes (Ed.), 2006, pp. 159–323.
- G. Schönhense, *J. Electron. Spectrosc. Relat. Phenom.* **137–140**, 769 (2004) .
- C.M. Schneider, G. Schönhense, *Rep. Prog. Phys.* **65**, R1785–R1839 (2002) .
- W. Kuch, in “*Magnetism: A Synchrotron Radiation Approach*”, Springer, Berlin, E. Beaurepaire *et al.* (Eds.), 2006, pp. 275–320.
- J. Feng, A. Scholl, in P.W. Hawkes, “*Science of Microscopy*”, Springer, New York, J.C.H. Spence (Eds.), 2007, pp. 657–695.
- E. Bauer and Th. Schmidt, in “*High Resolution Imaging and Spectroscopy of Materials*”, Springer, Berlin, Heidelberg, F. Ernst and M. Rühle (Eds.), 2002, pp. 363–390.
- E. Bauer, *J. Electron Spectrosc. Relat. Phenom.* **114–116**, 976–987 (2002).
- E. Bauer, *J. Phys.: Condens. Matter* **13**, 11391–11405 (2001).

Thank you for attention!



T. Onur Mentesh



Giovanni Zamborlini



Alessandro Sala

Theory group at ICTP (Trieste)

Nataša Stojić
Nadia Binggeli
Mighfar Imam
Chen Wang

STM group at IOM-CNR TASC laboratory

Laerte Patera
Cristina Africh
Giovanni Comelli